Electronic Supplementary Material (ESI) for New Journal of Chemistry.
This journal is © The Royal Society of Chemistry and the Centre National de la Recherche Scientifique 2020

SUPPORTING INFORMATION.

Copper(I) halides and palladium(II) chloride complexes of 4-thioxo[1,3,5]oxadiazocines: synthesis, structure and antibacterial activity

Andrey S. Kuzovlev,*[a] Daria A. Volkova,[a] Irina V. Parfenova,[a] Ivan V. Kulakov,[a] Alena O. Shkirdova,[b] Ilya A. Zamilatskov,[b] Vladimir V. Chernyshev,[b,c] Victor B. Rybakov,[c] Vladimir S. Tyurin[b], Nikolay N. Fefilov,[a] Alexey S. Vasilchenko[d]

[a] Dr. A. S. Kuzovlev, D. A. Volkova, I. V. Parfenova, Prof. Dr. I. V. Kulakov, N. N. Fefilov
Institute of Chemistry
University of Tyumen
Perekopskaya Str. 15a, 625003 Tyumen, Russian Federation
E-mail: a.s.kuzovlev@gmail.com

[b] A. O. Shkirdova, Dr. I. A. Zamilatskov, Dr. V. V. Chernyshev, Dr. Vladimir S. Tyurin
Laboratory of New Physicochemical Problems
A.N. Frumkin Institute of Physical chemistry and Electrochemistry RAS
Leninsky prospect 31-4, 119071 Moscow, Russian Federation

[c] Dr. V. V. Chernyshev, Dr. V. B. Rybakov
Department of Chemistry
M.V. Lomonosov Moscow State University
Leninskie Gory Str. 1-3, 119991 Moscow, Russian Federation

[d] Dr. A. S. Vasilchenko
Institute of Environmental and Agricultural Biology (X-BIO)
University of Tyumen
Lenina Str. 25, 625003 Tyumen, Russian Federation

Syntheses of ligands

4-thio-11-acetyl-2-methyl-4-thioxo-3,4,5,6-tetrahydro-2*H*-2,6-methanobenzo[*g*][1,3,5]oxadiazocine (L^1):[1] Mixture of acetylacetone (2.40 g, 24 mmol), finely ground thiourea (1.50 g, 20 mmol), salicylic aldehyde (2.44 g, 20 mmol) and trifluoroacetic acid (0.30 mL) in isopropyl alcohol (15 mL) was stirred at 50 °C for 2 hours, then at ambient temperature for 10 hours. The white precipitate was formed. The reaction mixture was filtered off and washed with cold isopropyl alcohol. The obtained crude material was two time recrystallized from isopropyl alcohol and dried in a desiccator for 1 d affording **L^1** (2.26 g, 43%) as a white powder: m.p.: 209-212 °C; Anal. Calcd for $C_{13}H_{14}N_2O_2S$ (%): C 59.52; H 5.38; N 10.68. Found (%): C 59.40; H 5.46; N 10.85; ^{1}H NMR (600 MHz, DMSO) δ 9.03 (s, 1H), 8.98 (d, *J* = 4.7 Hz, 1H), 7.24 – 7.20 (m, 2H), 6.96 – 6.93 (m, 1H), 6.83 (d, *J* = 8.1 Hz, 1H), 4.75 (dd, *J* = 5.2, 2.4 Hz, 1H), 3.43 (s, 1H), 2.28 (s, 3H), 1.69 (s, 3H); ^{13}C NMR (151 MHz, DMSO) δ 203.35, 176.49, 150.58, 129.58, 128.88, 124.22, 120.62, 116.35, 81.53, 48.04, 47.43, 29.12, 22.78; IR (Nujol): 3326, 3140, 3086, 1716, 1609, 1589, 1567, 1512, 1362, 1340, 1324, 1307, 1241, 1195, 1171, 1151, 1091, 965, 944, 916, 884, 864, 849, 833, 790, 760 cm^{-1}; UV-vis (λ_{max}, log ε) Et_2O: 202 (4.59), 265 (4.35); UV-vis (λ_{max}, log ε) CH_3CN: 192 (4.66), 260 (4.38).

Ethyl 2-methyl-4-thioxo-3,4,5,6-tetrahydro-2*H*-2,6-methanobenzo[*g*][1,3,5]oxadiazocine-11-carboxylate (L^2):[1] Mixture of ethyl acetoacetate (3.12 g, 24 mmol), finely ground thiourea (1.50 g, 20 mmol), salicylic aldehyde (2.44 g, 20 mmol) and trifluoroacetic acid (0.30 mL) in isopropyl alcohol (15 mL) was stirred at 50 °C for 2 hours, then at ambient temperature for 10 hours. The white precipitate was formed. The reaction mixture was filtered off and washed with cold isopropyl alcohol. The obtained crude material was two time recrystallized from isopropyl alcohol and dried in a desiccator for 1 d affording **L^2** (1.75 g, 30%) as a white powder: m.p.: 228-229 °C; Anal. Calcd for $C_{14}H_{16}N_2O_3S$ (%): C 57.52; H 5.52; N 9.58. Found (%): C 57.38; H 5.62; N 10.07; ^{1}H NMR (600 MHz, DMSO) δ 9.13 – 9.10 (m, 2H), 7.24 – 7.18 (m, 2H), 6.96 – 6.92 (m, 1H), 6.83 (d, *J* = 8.1 Hz, 1H), 4.58 (dd, *J* = 4.6, 2.5 Hz, 1H), 4.19 – 4.13 (m, 2H), 3.32 (s, 1H), 1.79 (s, 3H), 1.23 (t, *J* = 7.1 Hz, 3H); ^{13}C NMR (151 MHz, DMSO) δ 176.43, 167.78, 150.44, 129.64, 128.67, 123.69, 120.80, 116.35, 81.33, 60.69, 48.17, 42.29, 23.32, 13.94; IR (Nujol): 3326, 3185, 3097, 3047, 1723, 1609, 1588, 1565, 1509, 1491, 1396, 1352, 1331, 1321, 1297, 1270, 1253, 1229, 1204, 1189, 1178, 1152, 1115, 1087, 1069, 1028, 950, 913, 870, 858, 838, 809, 776, 759 cm^{-1}; UV-vis (λ_{max}, log ε) Et_2O: 220 (4.60), 264 (4.29).

1,2,3,4,9,9a-hexahydro-4a,9-(epiminomethanoimino)xanthene-12-thione (L^3):[2] Mixture of salicylaldehyde (7.33 g, 60 mmol), thiourea (4.72 g, 62 mmol), cyclohexanone (6.48 g, 66 mmol) and a few drops of hydrochloric acid (37%) in ethanol (40 mL) was refluxed for 5 hours. After completion of reaction, monitored by TLC, the reaction mixture was cooled to room temperature, the reaction mixture was filtered off and washed with cold ethanol. The obtained crude material was two time recrystallized from isopropyl alcohol and dried in a desiccator for 1 d affording **L^3** (9.84 g, 63%) as a white powder: m.p.: 256-257 °C; Anal. Calcd for $C_{14}H_{16}N_2OS$ (%): C 64.59; H 6.19; N 10.76. Found (%): C 64.25; H 6.53; N 10.92; ^{1}H NMR (600 MHz, DMSO) δ 8.99 (s, 1H), 8.78 (s, 1H), 7.20 – 7.16 (m, 1H), 7.11 (d, *J* = 6.6 Hz, 1H), 6.91 – 6.86 (m, 1H), 6.79 (d, *J* = 8.1 Hz, 1H), 4.05 (d, *J* = 2.1 Hz, 1H), 2.33 (d, *J* = 12.7 Hz, 1H), 2.00 (d, *J* = 11.4 Hz, 1H), 1.73 – 1.64 (m, 4H), 1.37 – 1.27 (m, 2H), 1.15 – 1.07 (m, 1H); ^{13}C NMR (151 MHz, DMSO) δ 175.84, 150.68, 129.12, 128.76, 125.25, 120.22, 116.16, 82.81, 48.93, 34.29, 33.74, 24.56, 23.60, 22.09; IR (Nujol): 3357, 3180, 3062, 1606, 1584, 1552, 1488, 1415, 1356, 1337, 1320, 1295, 1250, 1231, 1220, 1190, 1157, 1149, 1104, 1059, 1036, 1024, 998, 954, 932, 877, 854, 835, 793, 768, 753, 742 cm^{-1}; UV-vis (λ_{max}, log ε) CH_3CN: 196 (4.55), 259 (4.34).

Crystal Structure Determination

Single crystals of compound **1** suitable for crystal structure analysis were obtained after crystallization from acetonitrile under reduced pressure at room temperature. The intensity data set was collected at room temperature using a Stoe STADI VARI diffractometer (Cu K_a radiation, l = 1.54186 Å). The crystal structure was solved by direct methods with the *SHELXS* program and refined by full-matrix least-squares on F^2 with *SHELXL*.[3] Hydrogen atoms were placed geometrically and refined using a riding model with U_{iso} constrained at 1.2-1.5 times U_{eq} of the carrier C or N atoms. Graphic representation of the structures was prepared with *PLATON*[4] and *Mercury*.[5] The crystal data, data collection and refinement parameters are given in Table S1.

The molecular structure of compound **4** was confirmed by X-ray structure determination from powder data measured at room temperature on the laboratory diffractometer EMPYREAN (Panalytical) with a linear Xcelerator detector using nonmonochromated CuK_a radiation. The powder pattern was indexed in a monoclinic unit cell, and the crystal structure was solved with the use of simulated annealing technique and refined with the program MRIA following the known procedure described by us earlier.[6] The crystal data, data collection and refinement parameters are given in Table 6. The diffraction profile after the final bond-restrained Rietveld refinement is shown in Figure S1.

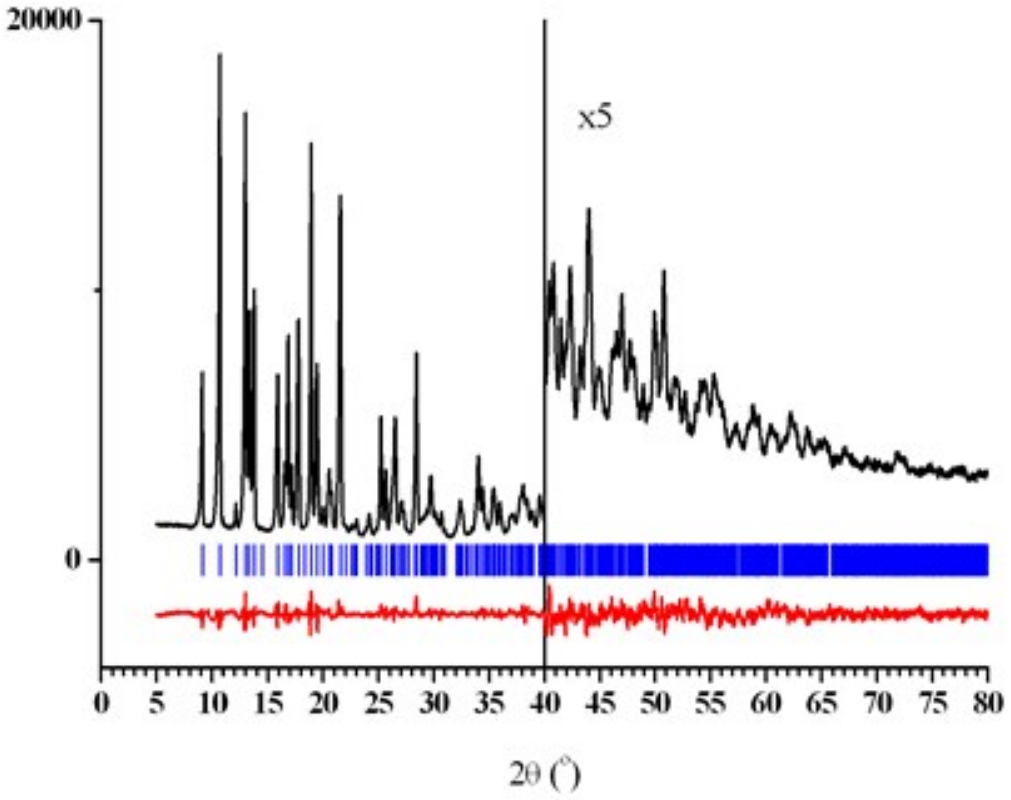

Figure S1. The final Rietveld plot for compound $[Pd(L^1)_2Cl_2]$. The experimental and difference (experimental minus calculated) diffraction profiles are shown as the black and red lines, respectively. The vertical blue bars correspond to the calculated positions of the Bragg peaks.

Table S1. Crystal data for complexes

Compound	**[Cu(L^1)$_2$Cl]** (**1**)	**[Pd(L^1)$_2$Cl$_2$]** (**4**)
sample	single-crystal	powder
empirical formula	$C_{26}H_{28}ClCuN_4O_4S_2$	$C_{26}H_{28}Cl_2N_4O_4PdS_2$
M_r	623.64	701.94
crystal size, mm^3	0.12 x 0.10 x 0.09	
crystal form, color	prism, colorless	
crystal system	Monoclinic	Monoclinic
space group	P21/c	P21/n
diffractometer	Stoe STADI VARI	EMPYREAN
wavelength, Å	1.5418	1.5418
unit cell dimensions:		
a, Å	15.8162(10)	9.3909(8)
b, Å	10.0508(5)	19.3472(17)
c, Å	17.7915(12)	8.1182(8)
β, º	94.782(5)	103.842(11)
volume, Å^3	2818.4(3)	1432.1(2)
Z	4	2
Dx (Mg m^{-3})	1.470	1.628
μ, mm-1	3.678	8.642
2θmin-2θmax, Δ2θ (º)		5.008 – 80.007, 0.017
no. reflections collected/independent	23672/5497 [R(int) = 0.0617]	
no. parameters/restraints	343	107/67
GOF	0.744	
final R indices [I>2σ(I)]	R = 0.047 wR = 0.0997	
Rp, Rwp, Rexp		0.0337, 0.0434, 0.0250

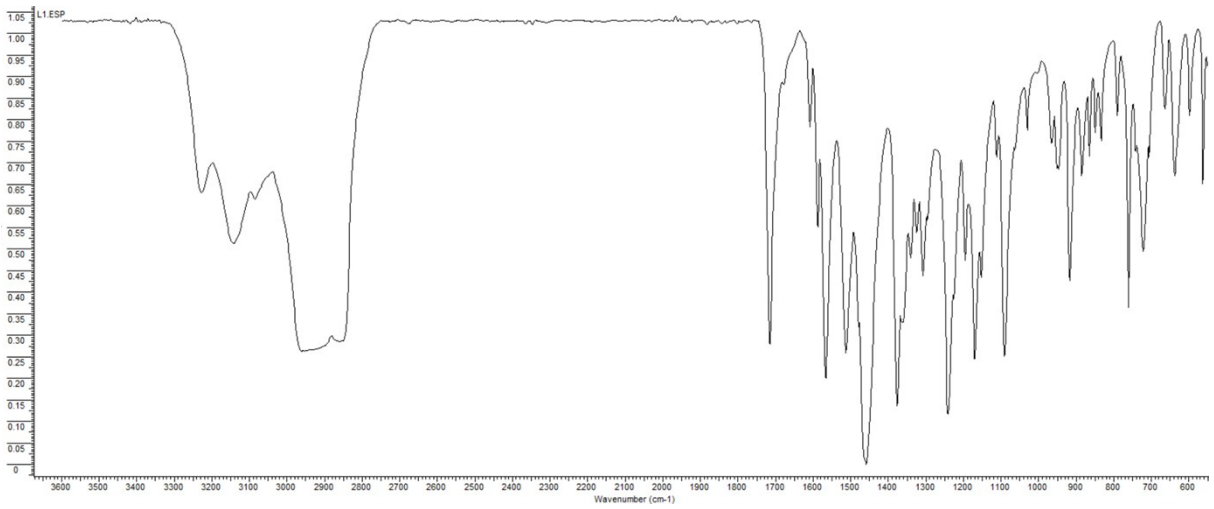

Figure S2. FTIR of 11-acetyl-2-methyl-4-thioxo-3,4,5,6-tetrahydro-2*H*-2,6-methanobenzo[*g*][1,3,5]oxadiazocine (L^1)

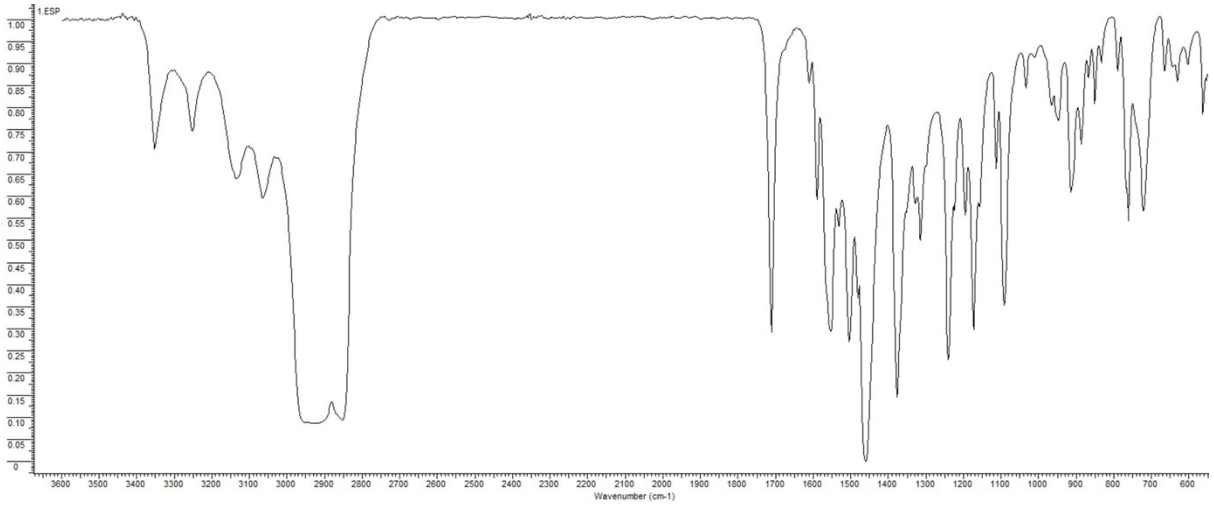

Figure S3. FTIR of chlorobis(11-acetyl-2-methyl-4-thioxo-3,4,5,6-tetrahydro-2*H*-2,6-methanobenzo[*g*][1,3,5]oxadiazocine) copper(I), $[Cu(L^1)_2Cl]$ (1)

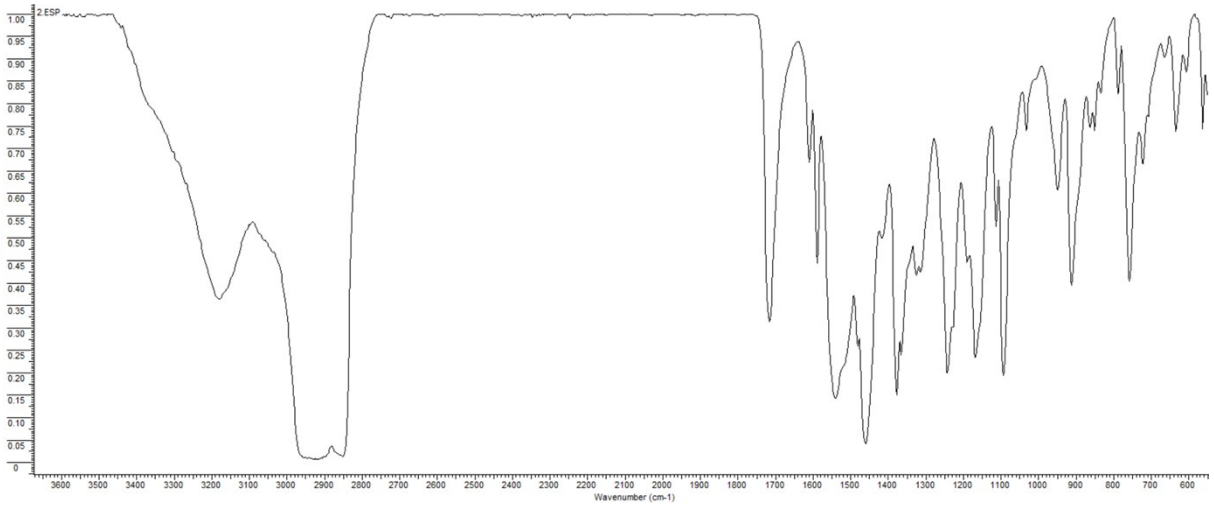

Figure S4. FTIR of bromobis(11-acetyl-2-methyl-4-thioxo-3,4,5,6-tetrahydro-2*H*-2,6-methanobenzo[*g*][1,3,5]oxadiazocine) copper(I), $[Cu(L^1)_2Br]$ (2)

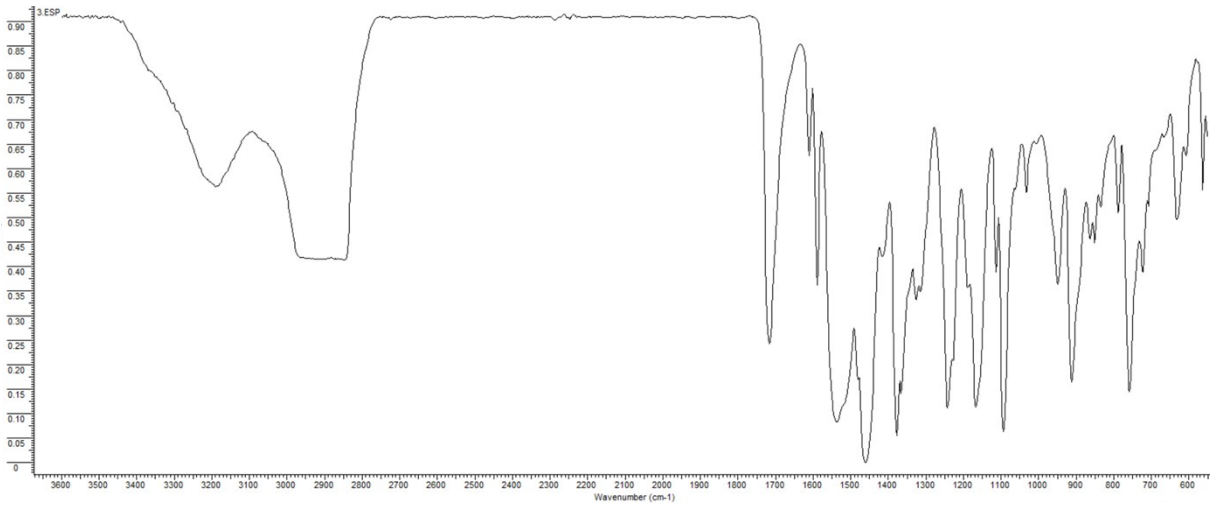

Figure S5. FTIR of iodobis(11-acetyl-2-methyl-4-thioxo-3,4,5,6-tetrahydro-2*H*-2,6-methanobenzo[*g*][1,3,5]oxadiazocine) copper(I), $[Cu(L^1)_2I]$ (3)

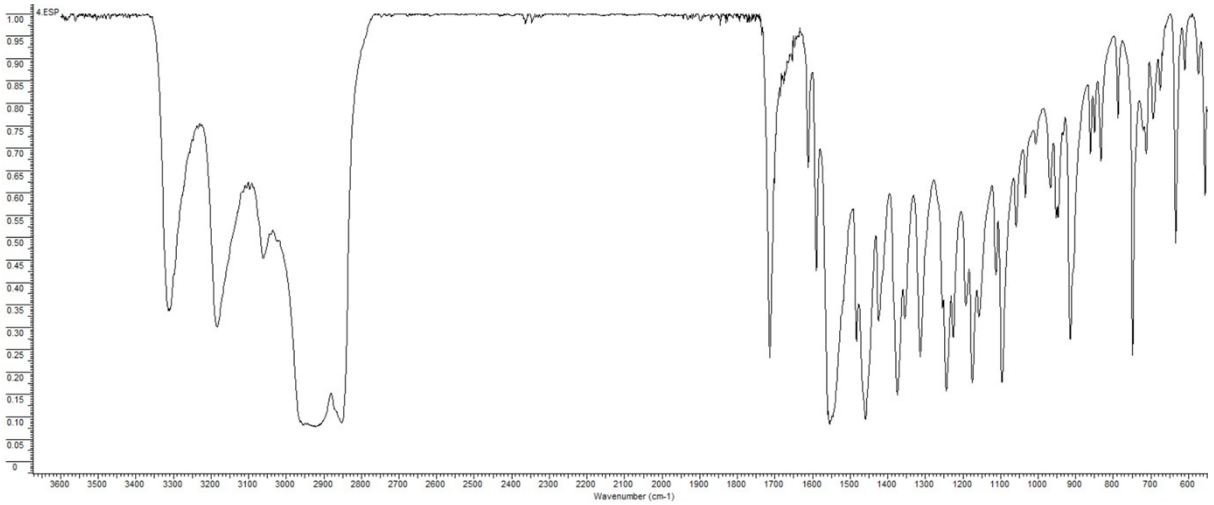

Figure S6. FTIR of dichlorobis(11-acetyl-2-methyl-4-thioxo-3,4,5,6-tetrahydro-2*H*-2,6-methanobenzo[*g*][1,3,5]oxadiazocine) palladium(II), $[Pd(L^1)_2Cl_2]$ (4)

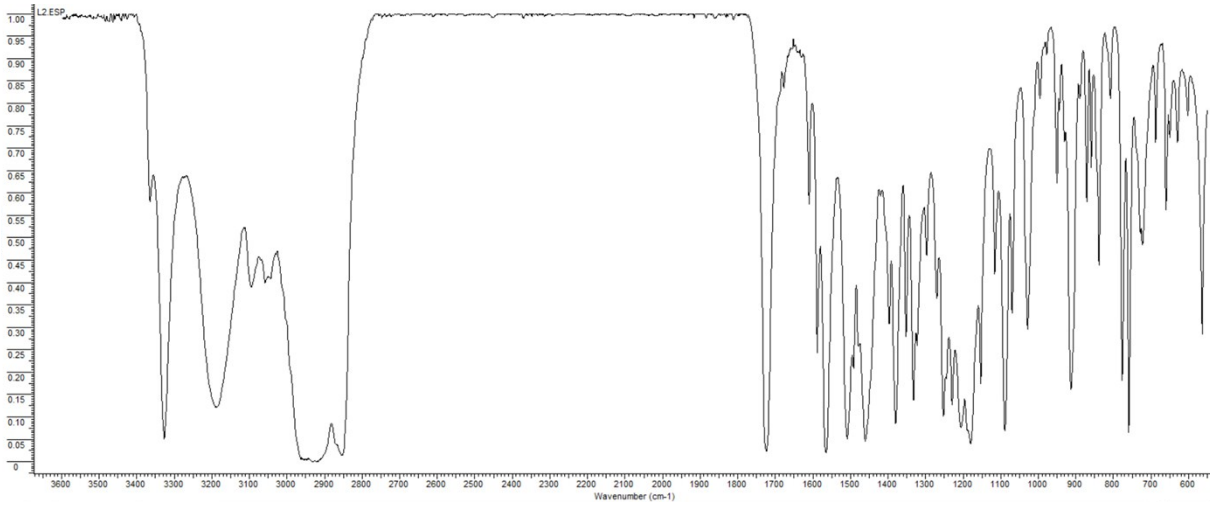

Figure S7. FTIR of ethyl 2-methyl-4-thioxo-3,4,5,6-tetrahydro-2*H*-2,6-methanobenzo[*g*][1,3,5]oxadiazocine-11-carboxylate (L^2)

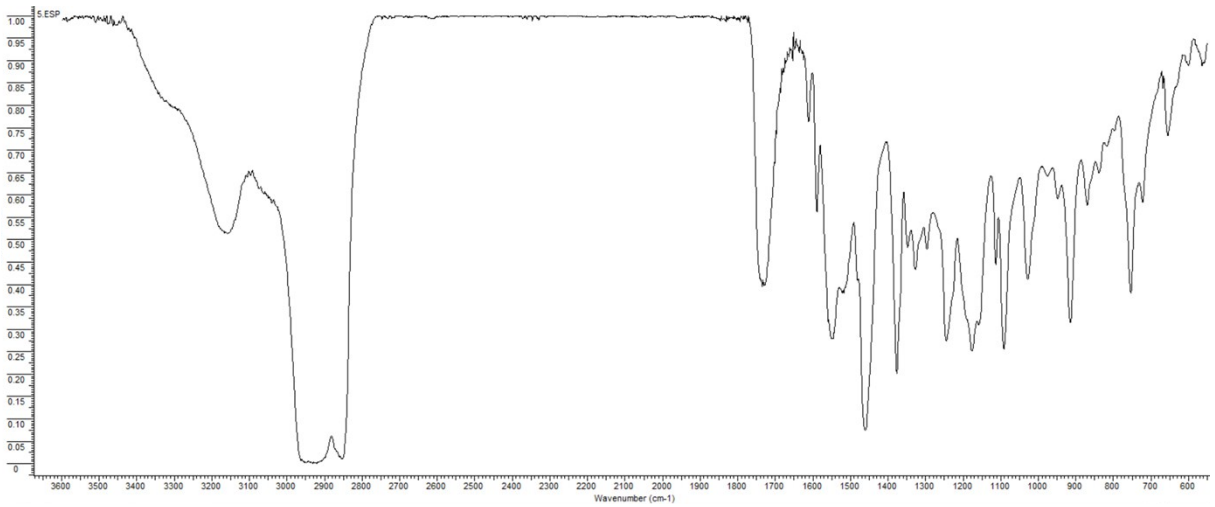

Figure S8. FTIR of chlorobis(ethyl 2-methyl-4-thioxo-3,4,5,6-tetrahydro-2*H*-2,6-methanobenzo[*g*][1,3,5]oxadiazocine-11-carboxylate)copper(I), $[Cu(L^2)_2Cl]$ (5)

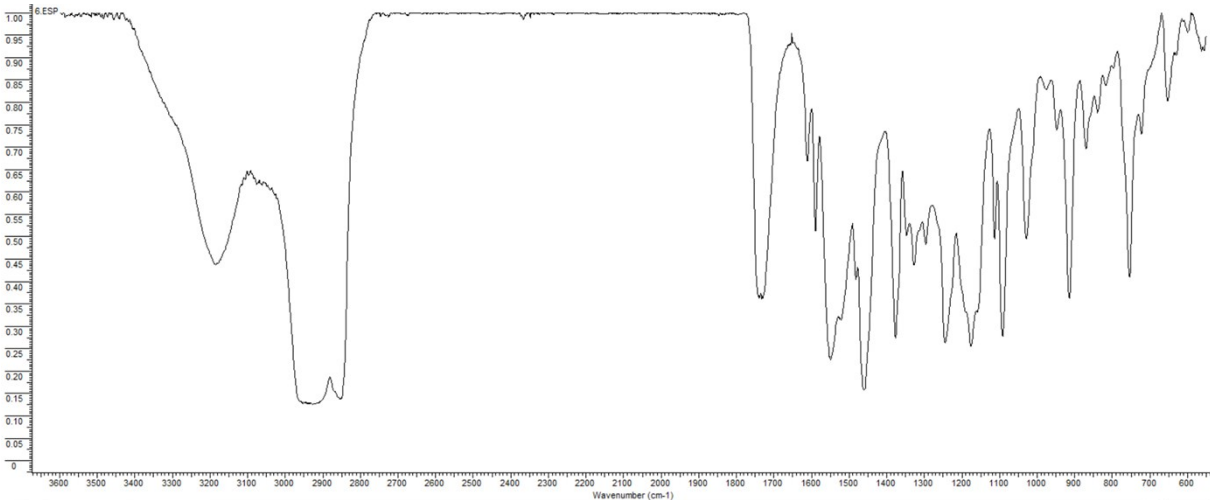

Figure S9. FTIR of bromobis(ethyl 2-methyl-4-thioxo-3,4,5,6-tetrahydro-2*H*-2,6-methanobenzo[*g*][1,3,5]oxadiazocine-11-carboxylate)copper(I), $[Cu(L^2)_2Br]$ (6)

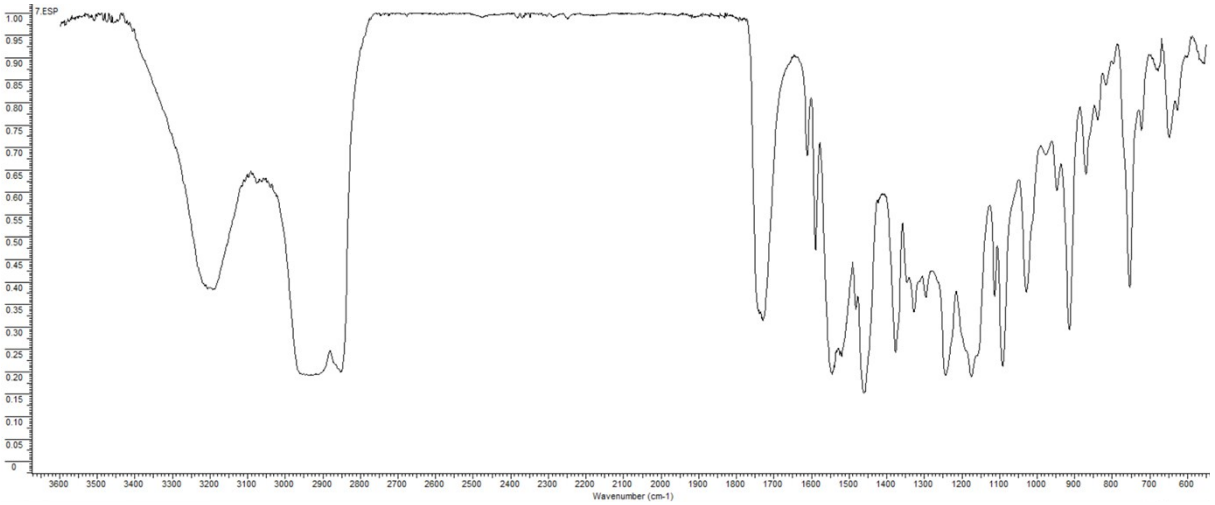

Figure S10. FTIR of iodobis(ethyl 2-methyl-4-thioxo-3,4,5,6-tetrahydro-2*H*-2,6-methanobenzo[*g*][1,3,5]oxadiazocine-11-carboxylate)copper(I), $[Cu(L^2)_2I]$ (7)

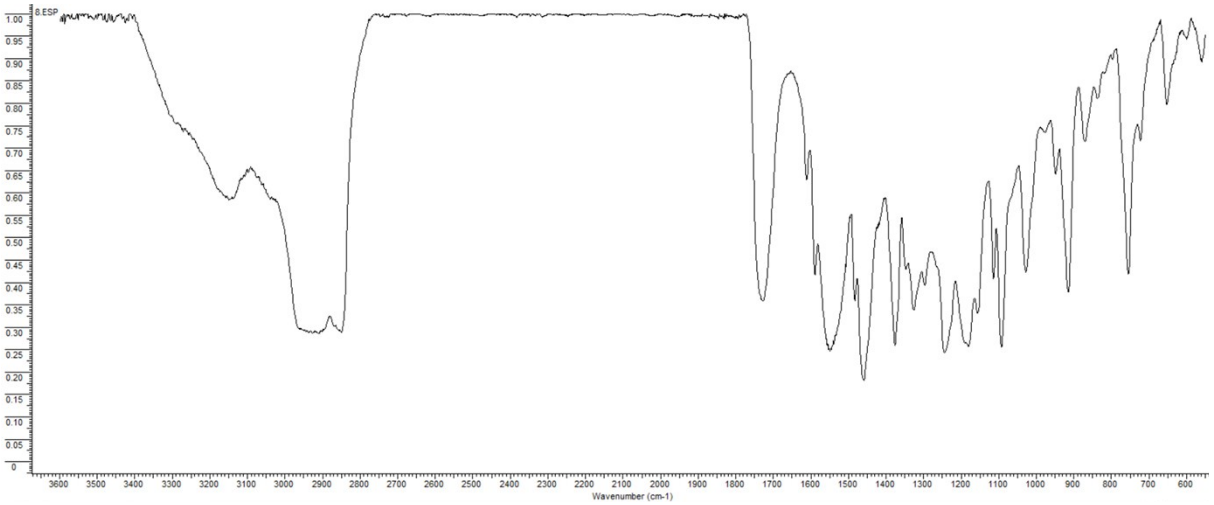

Figure S11. FTIR of dichlorobis(ethyl 2-methyl-4-thioxo-3,4,5,6-tetrahydro-2*H*-2,6-methanobenzo[*g*][1,3,5]oxadiazocine-11-carboxylate)palladium(II), $[Pd(L^2)_2Cl_2]$ (8)

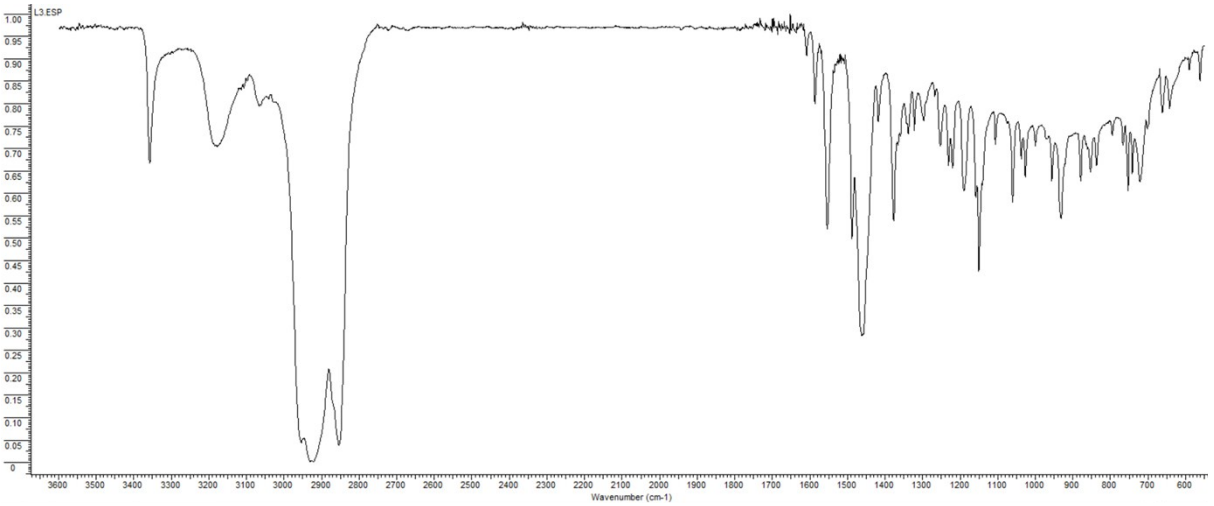

Figure S12. FTIR of 1,2,3,4,9,9a-hexahydro-4a,9-(epiminomethanoimino)xanthene-12-thione (L^3)

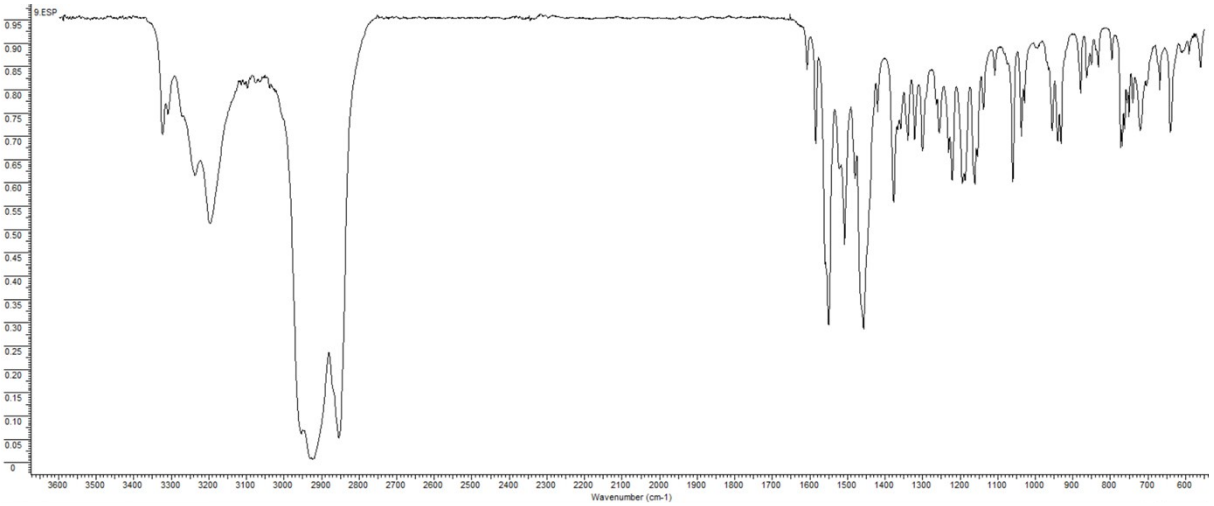

Figure S13. FTIR of chlorobis(1,2,3,4,9,9a-hexahydro-4a,9-(epiminomethanoimino)xanthene-12-thione)copper(I), $[Cu(L^3)_2Cl]$ (9)

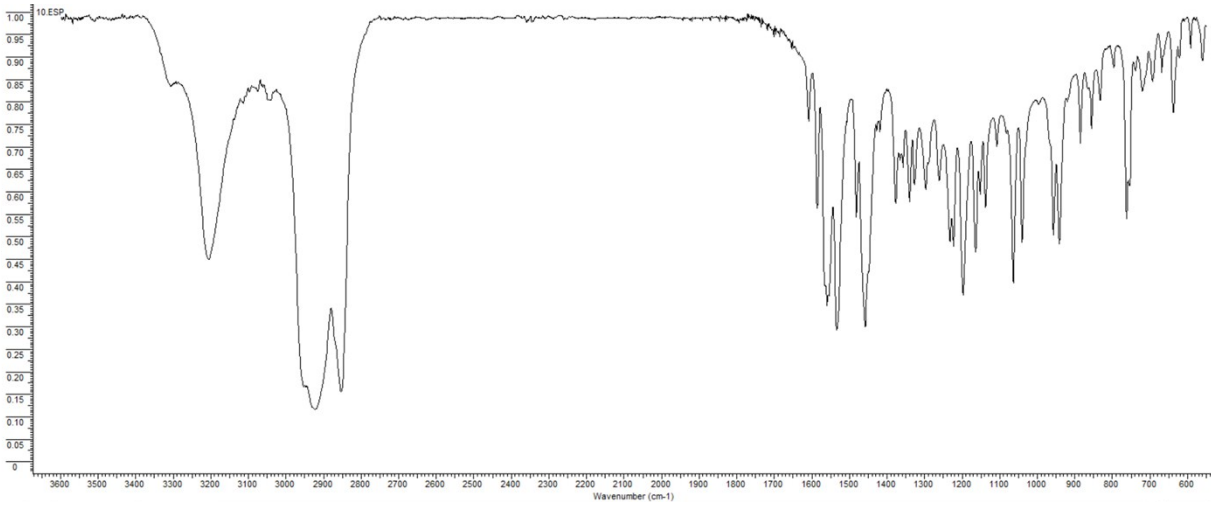

Figure S14. FTIR of bromobis(1,2,3,4,9,9a-hexahydro-4a,9-(epiminomethanoimino)xanthene-12-thione)copper(I), $[Cu(L^3)_2Br]$ (10)

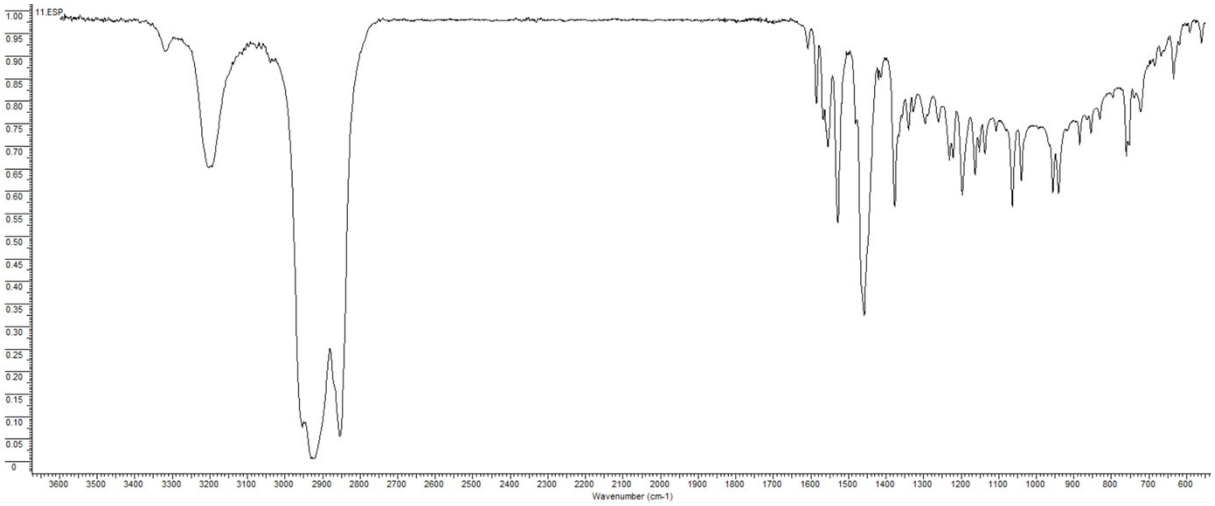

Figure S15. FTIR of iodobis(1,2,3,4,9,9a-hexahydro-4a,9-(epiminomethanoimino)xanthene-12-thione)copper(I), $[Cu(L^3)_2I]$ (11)

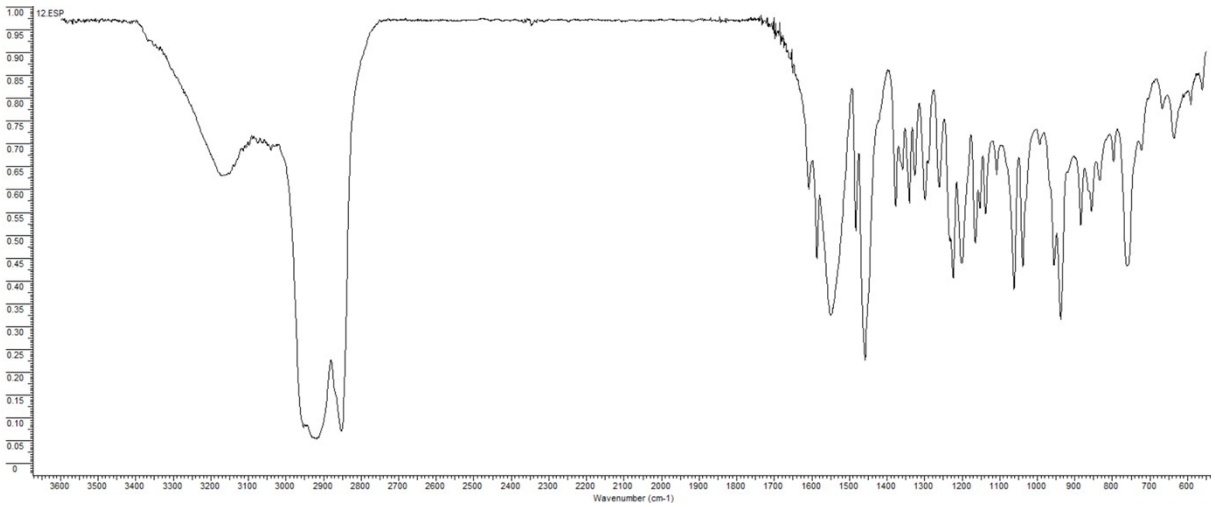

Figure S16. FTIR of dichlorobis(1,2,3,4,9,9a-hexahydro-4a,9-(epiminomethanoimino)xanthene-12-thione)palladium(II), $[Pd(L^3)_2Cl_2]$ (12)

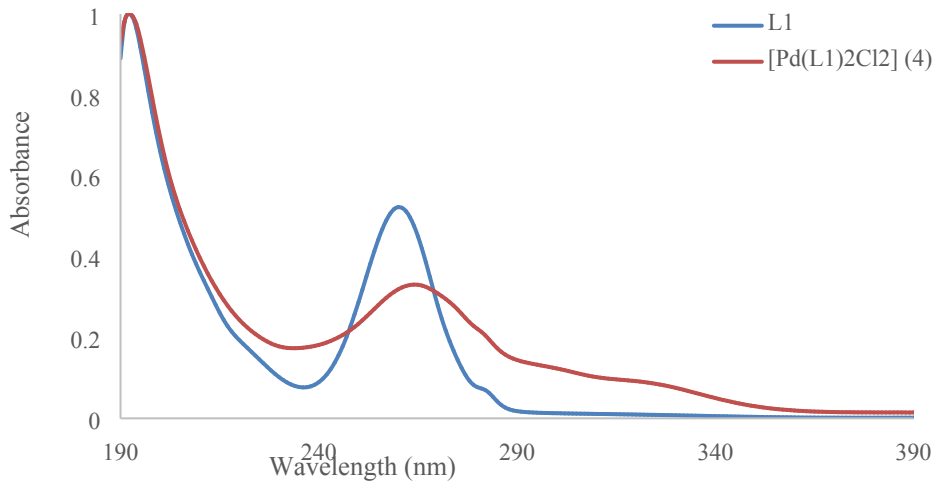

Figure S17. UV-vis of L^1 and $[Pd(L^1)_2Cl_2]$ (4) in CH_3CN

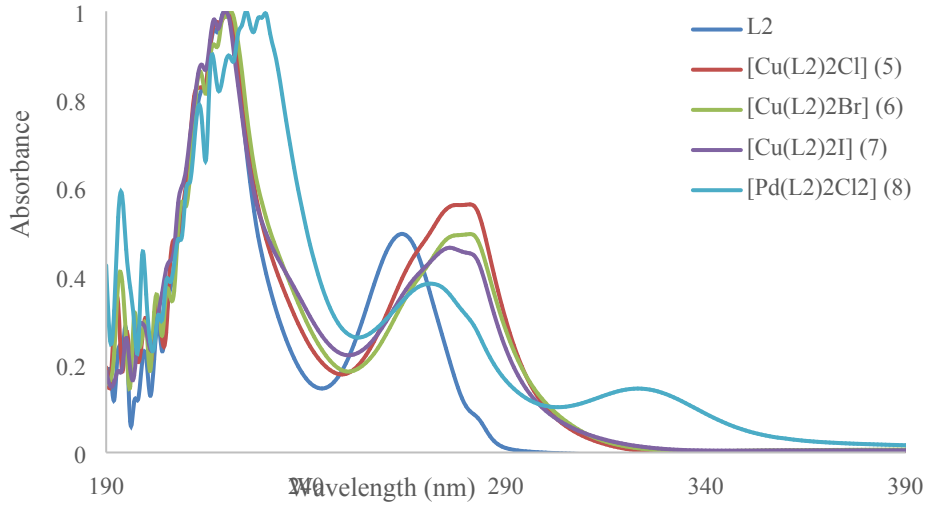

Figure S18. UV-vis of L^2, $[Cu(L^2)2Cl]$ (5), $[Cu(L^2)_2Br]$ (6), $[Cu(L^2)_2I]$ (7) and $[Pd(L^2)_2Cl_2]$ (8) in Et_2O

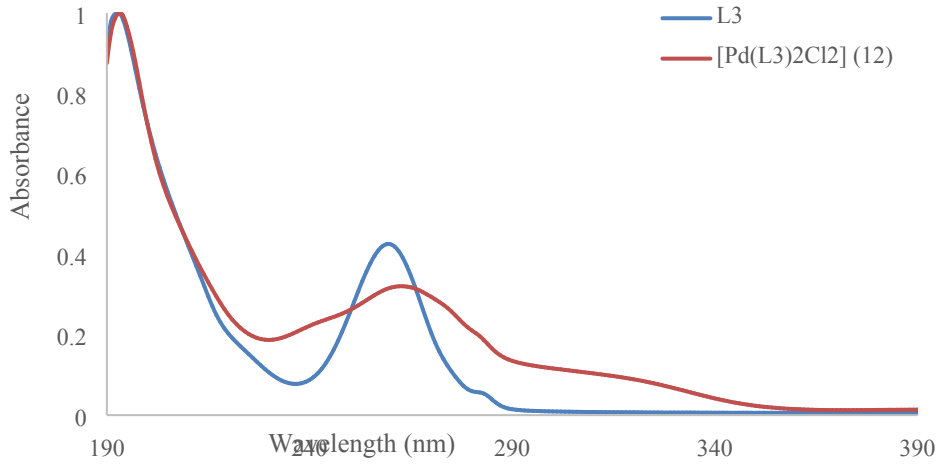

Figure S19. UV-vis of L^3 and $[Pd(L^3)_2Cl_2]$ (12) in CH_3CN

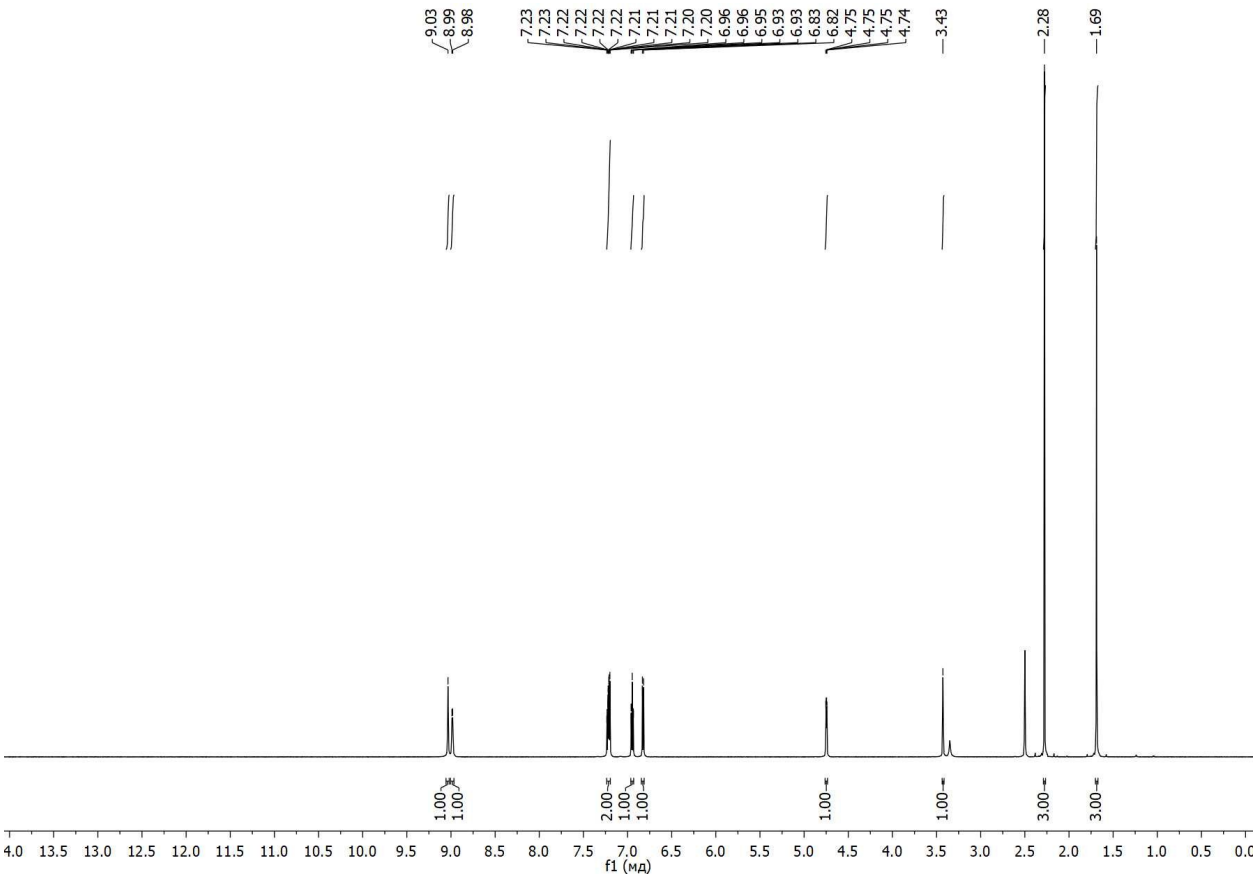

Figure S20. ^{1}H-NMR of 11-acetyl-2-methyl-4-thioxo-3,4,5,6-tetrahydro-2*H*-2,6-methanobenzo[*g*][1,3,5]oxadiazocine (L^1)

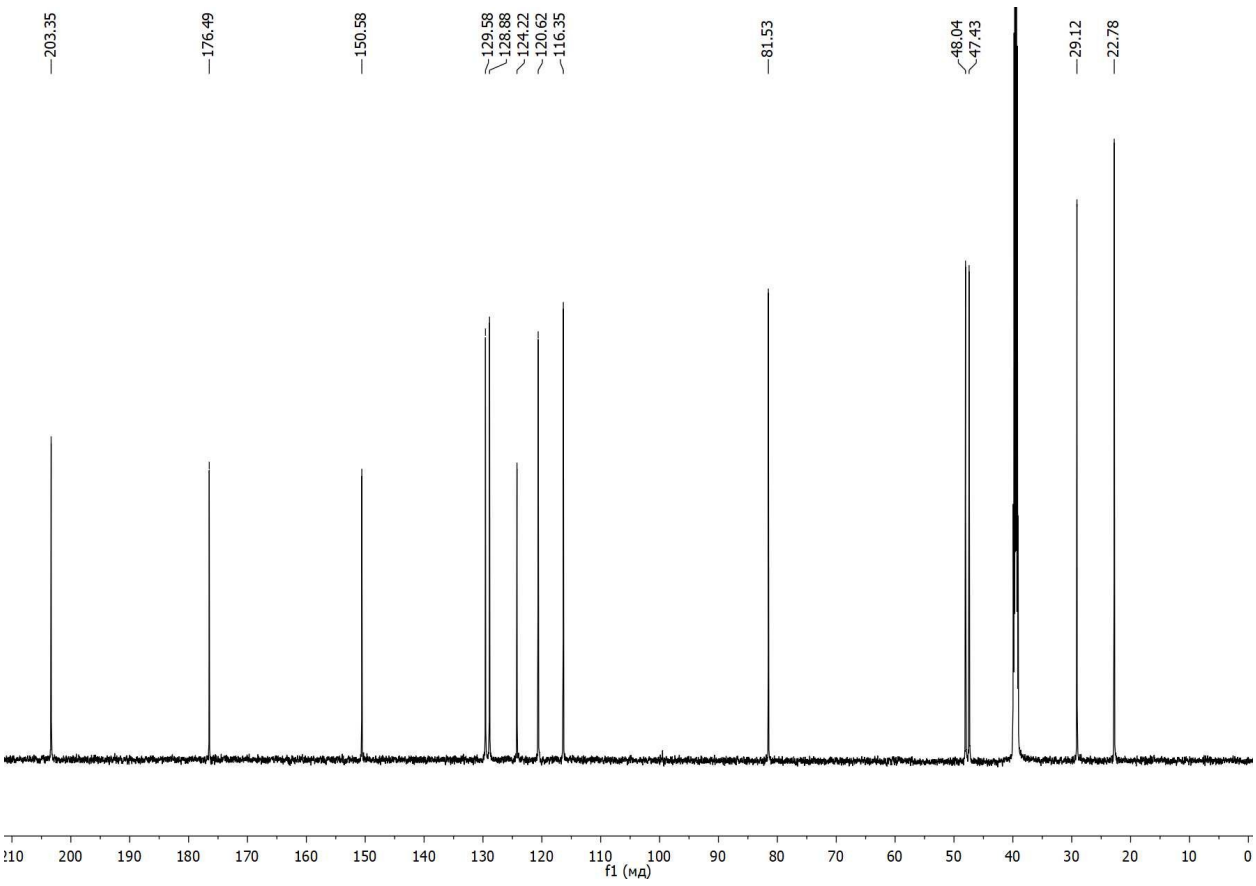

Figure S21. ^{13}C-NMR of 11-acetyl-2-methyl-4-thioxo-3,4,5,6-tetrahydro-2*H*-2,6-methanobenzo[*g*][1,3,5]oxadiazocine (L^1)

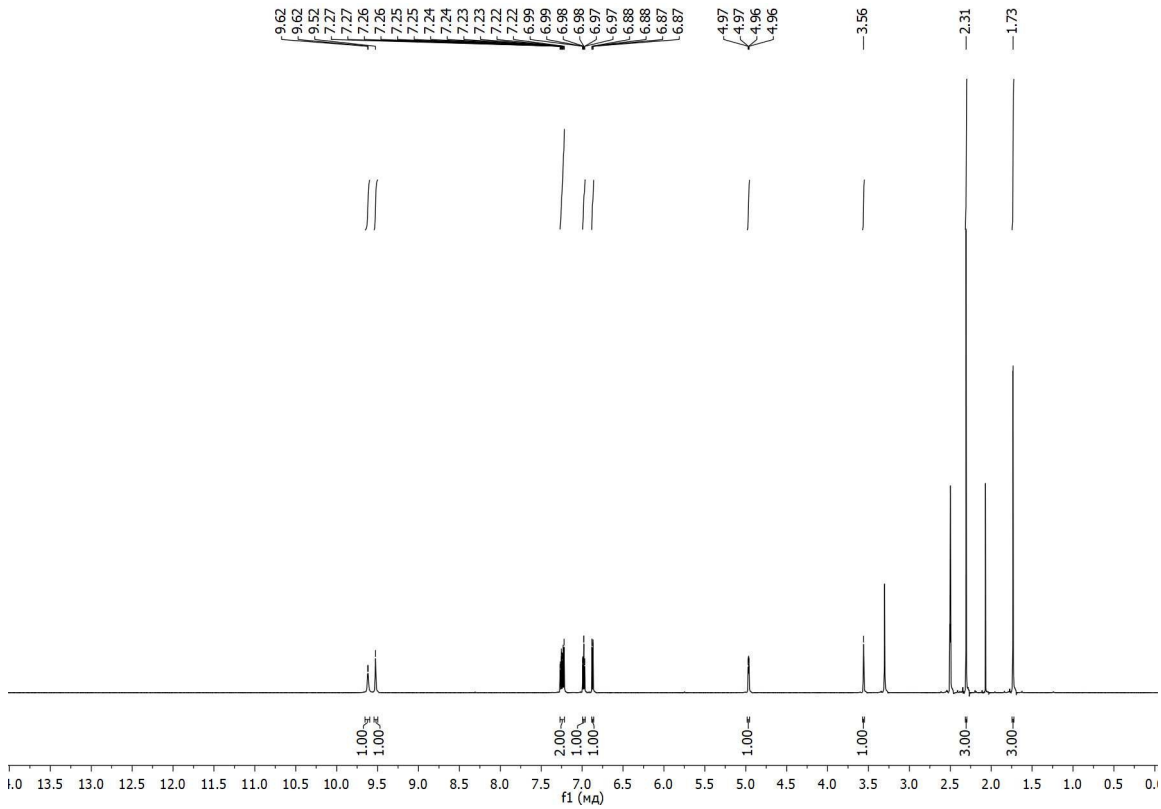

Figure S22. ^{1}H-NMR of chlorobis(11-acetyl-2-methyl-4-thioxo-3,4,5,6-tetrahydro-2*H*-2,6-methanobenzo[*g*][1,3,5]oxadiazocine) copper(I), [Cu(L^{1})$_2$Cl] (1)

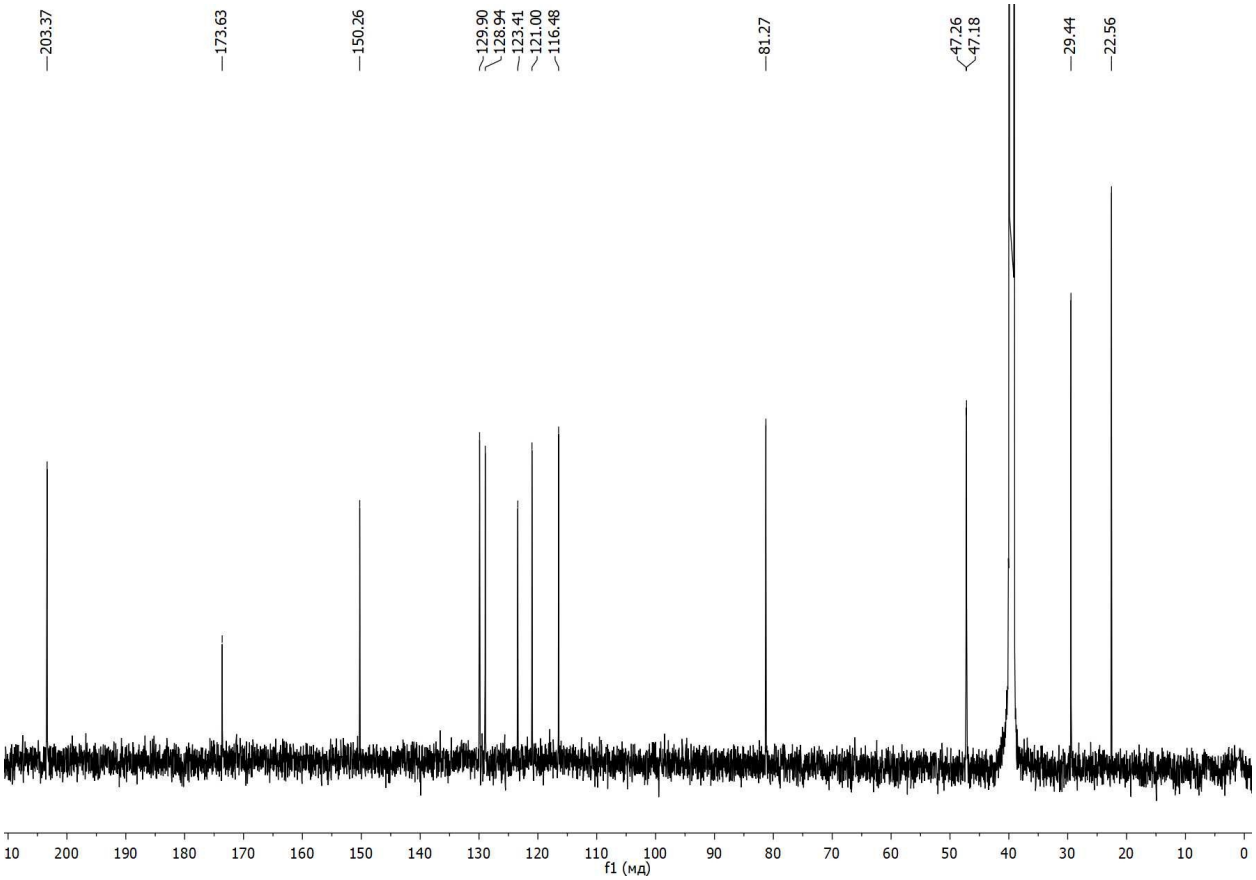

Figure S23. ^{13}C-NMR of chlorobis(11-acetyl-2-methyl-4-thioxo-3,4,5,6-tetrahydro-2*H*-2,6-methanobenzo[*g*][1,3,5]oxadiazocine) copper(I), [Cu(L^{1})$_2$Cl] (1)

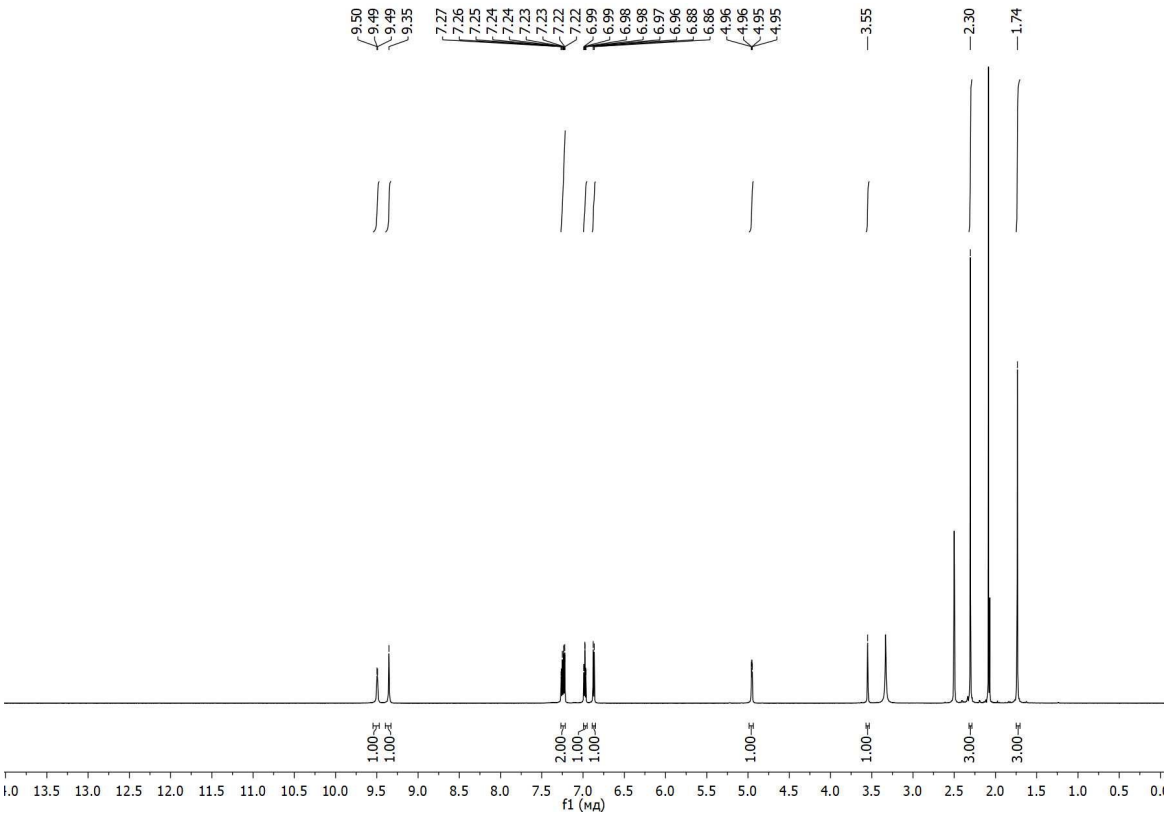

Figure S24. ^{1}H-NMR of bromobis(11-acetyl-2-methyl-4-thioxo-3,4,5,6-tetrahydro-2*H*-2,6-methanobenzo[*g*][1,3,5]oxadiazocine) copper(I), [Cu(L^1)$_2$Br] (2)

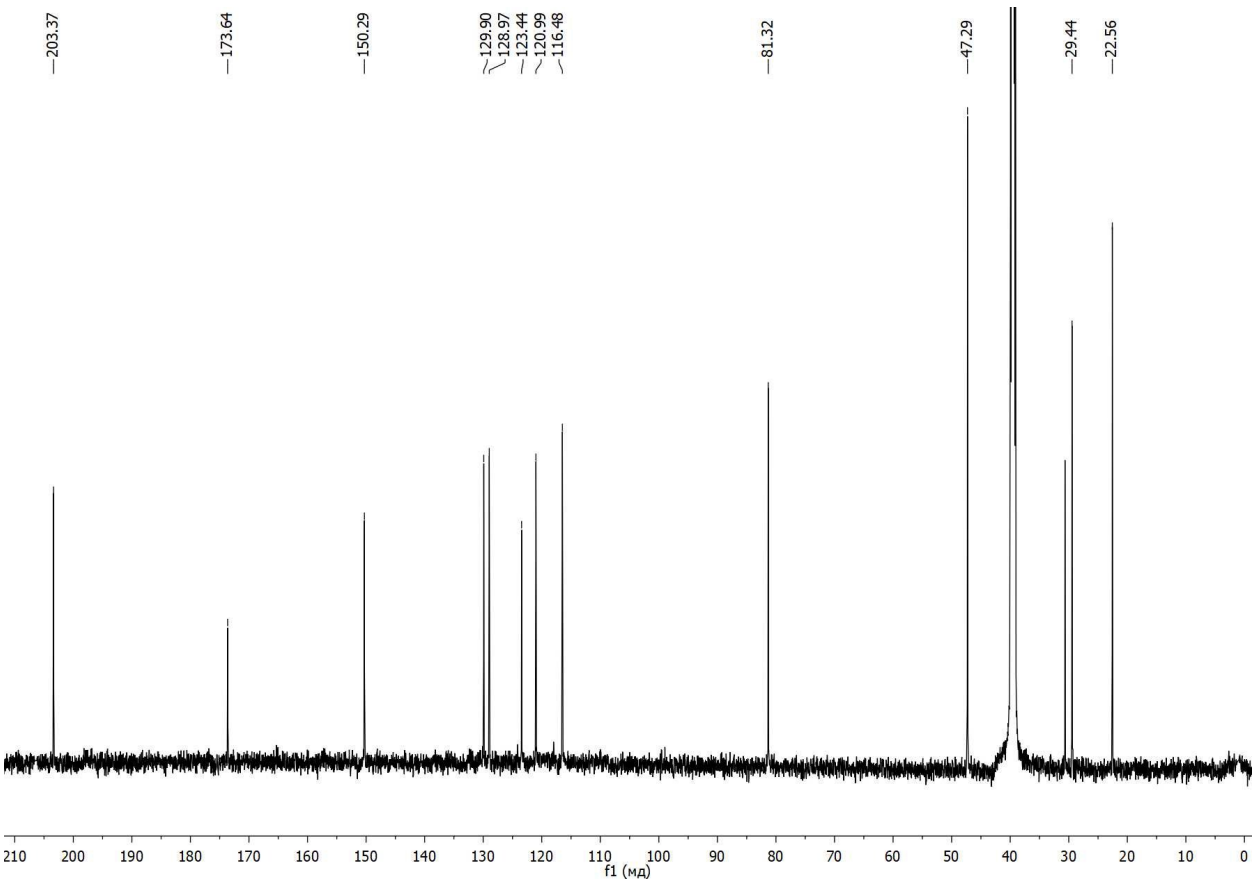

Figure S25. ^{13}C-NMR of bromobis(11-acetyl-2-methyl-4-thioxo-3,4,5,6-tetrahydro-2*H*-2,6-methanobenzo[*g*][1,3,5]oxadiazocine) copper(I), [Cu(L^1)$_2$Br] (2)

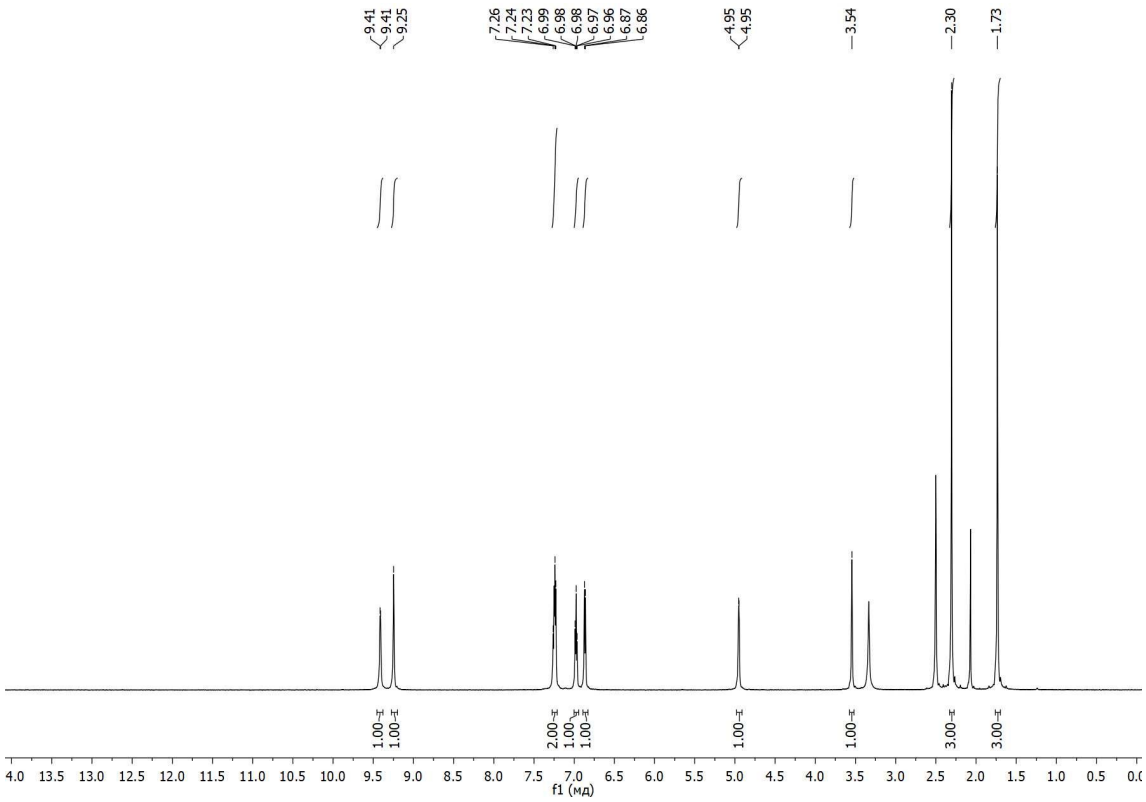

Figure S26. ^{1}H-NMR of iodobis(11-acetyl-2-methyl-4-thioxo-3,4,5,6-tetrahydro-2*H*-2,6-methanobenzo[*g*][1,3,5]oxadiazocine) copper(I), [Cu(L^1)$_2$I] (3)

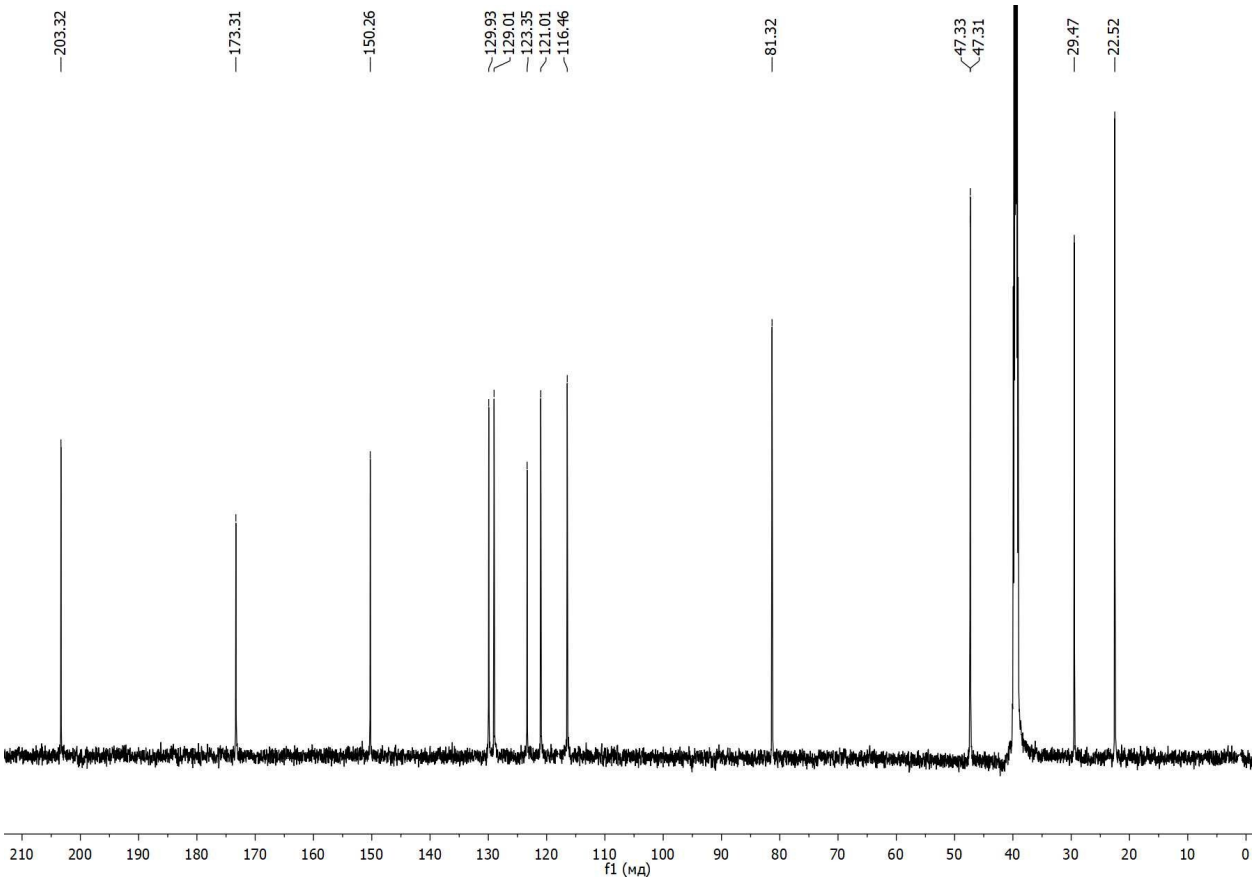

Figure S27. ^{13}C-NMR of iodobis(11-acetyl-2-methyl-4-thioxo-3,4,5,6-tetrahydro-2*H*-2,6-methanobenzo[*g*][1,3,5]oxadiazocine) copper(I), [Cu(L^1)$_2$I] (3)

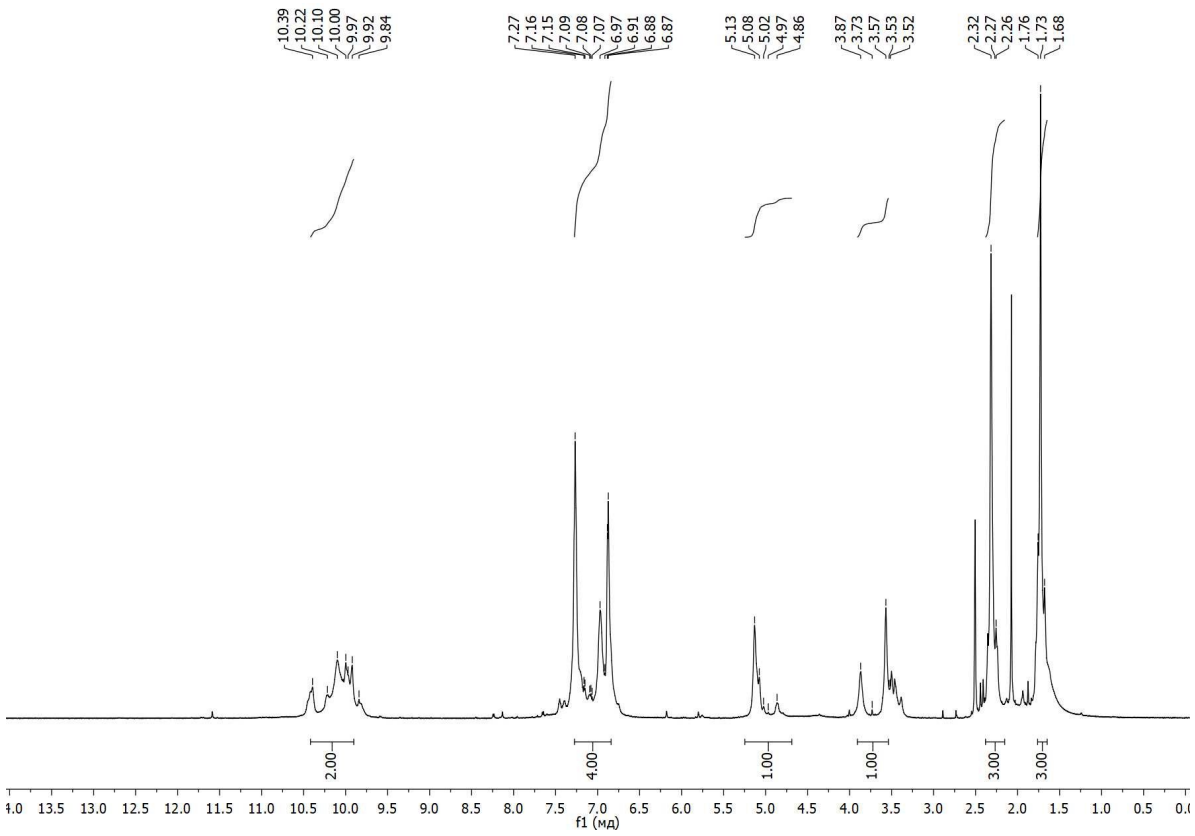

Figure S28. ^{1}H-NMR of dichlorobis(11-acetyl-2-methyl-4-thioxo-3,4,5,6-tetrahydro-2*H*-2,6-methanobenzo[*g*][1,3,5]oxadiazocine) palladium(II), $[Pd(L^1)_2Cl_2]$ (4)

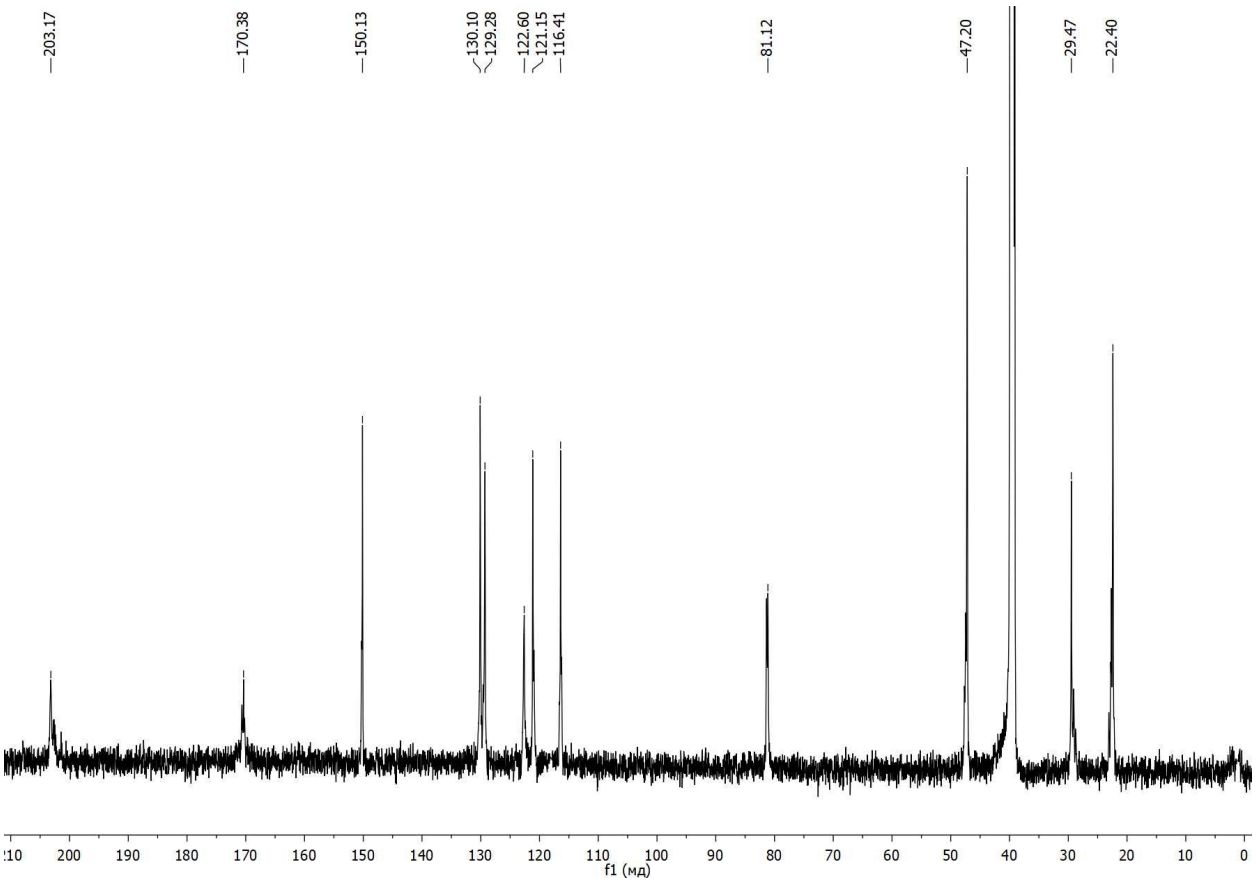

Figure S29. ^{13}C-NMR of dichlorobis(11-acetyl-2-methyl-4-thioxo-3,4,5,6-tetrahydro-2*H*-2,6-methanobenzo[*g*][1,3,5] oxadiazocine) palladium(II), $[Pd(L^1)_2Cl_2]$ (4)

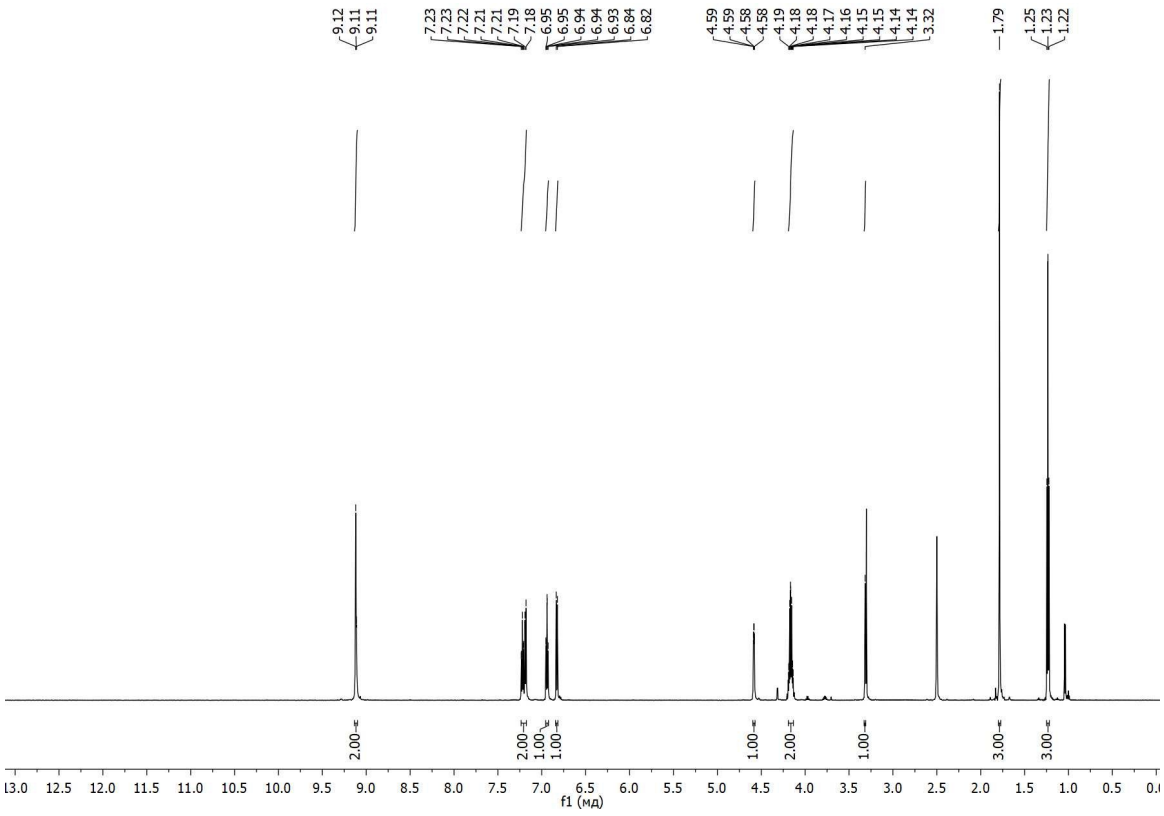

Figure S30. ^{1}H-NMR of ethyl 2-methyl-4-thioxo-3,4,5,6-tetrahydro-2*H*-2,6-methanobenzo[*g*][1,3,5]oxadiazocine-11-carboxylate (L^2)

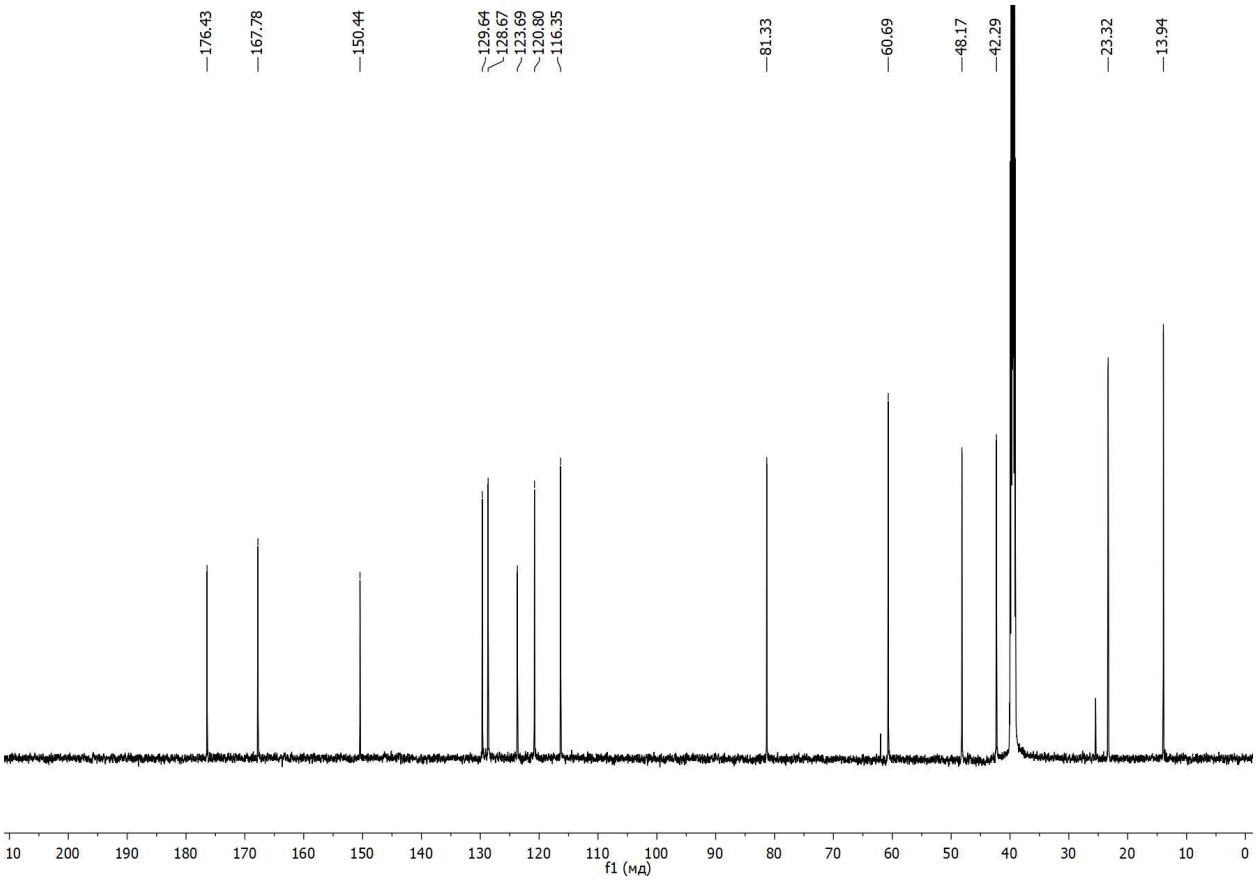

Figure S31. ^{13}C-NMR of ethyl 2-methyl-4-thioxo-3,4,5,6-tetrahydro-2*H*-2,6-methanobenzo[*g*][1,3,5]oxadiazocine-11-carboxylate (L^2)

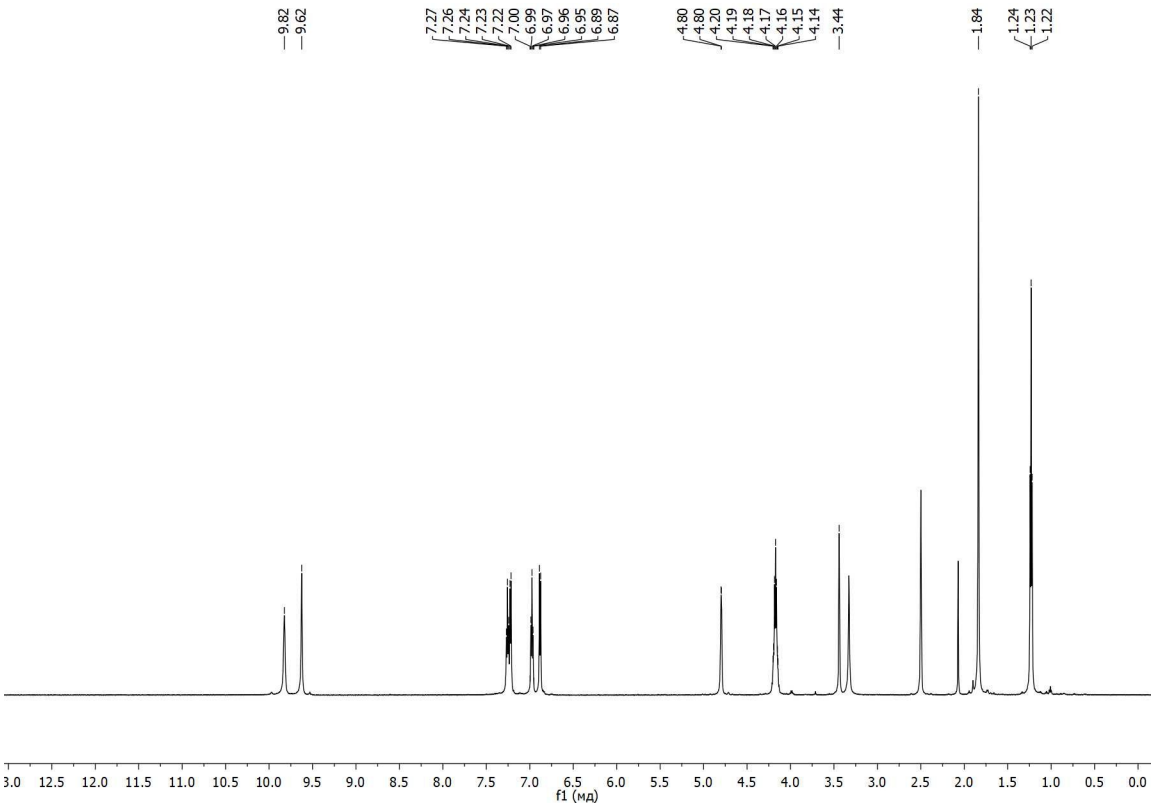

Figure S32. ^{1}H-NMR of chlorobis(ethyl 2-methyl-4-thioxo-3,4,5,6-tetrahydro-2*H*-2,6-methanobenzo[*g*][1,3,5]oxadiazocine-11-carboxylate)copper(I), [Cu(L^2)$_2$Cl] (5)

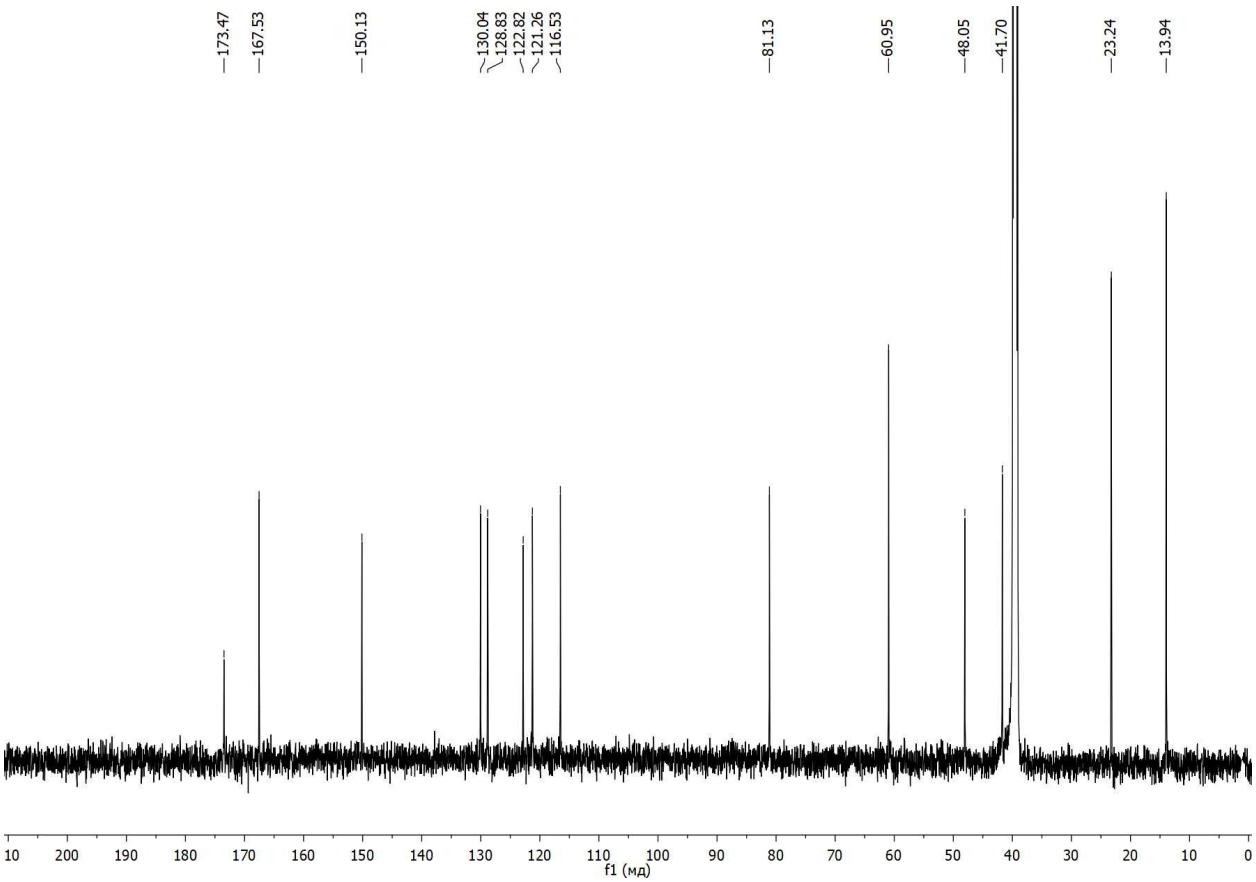

Figure S33. ^{13}C-NMR of chlorobis(ethyl 2-methyl-4-thioxo-3,4,5,6-tetrahydro-2*H*-2,6-methanobenzo[*g*][1,3,5]oxadiazocine-11-carboxylate)copper(I), [Cu(L^2)$_2$Cl] (5)

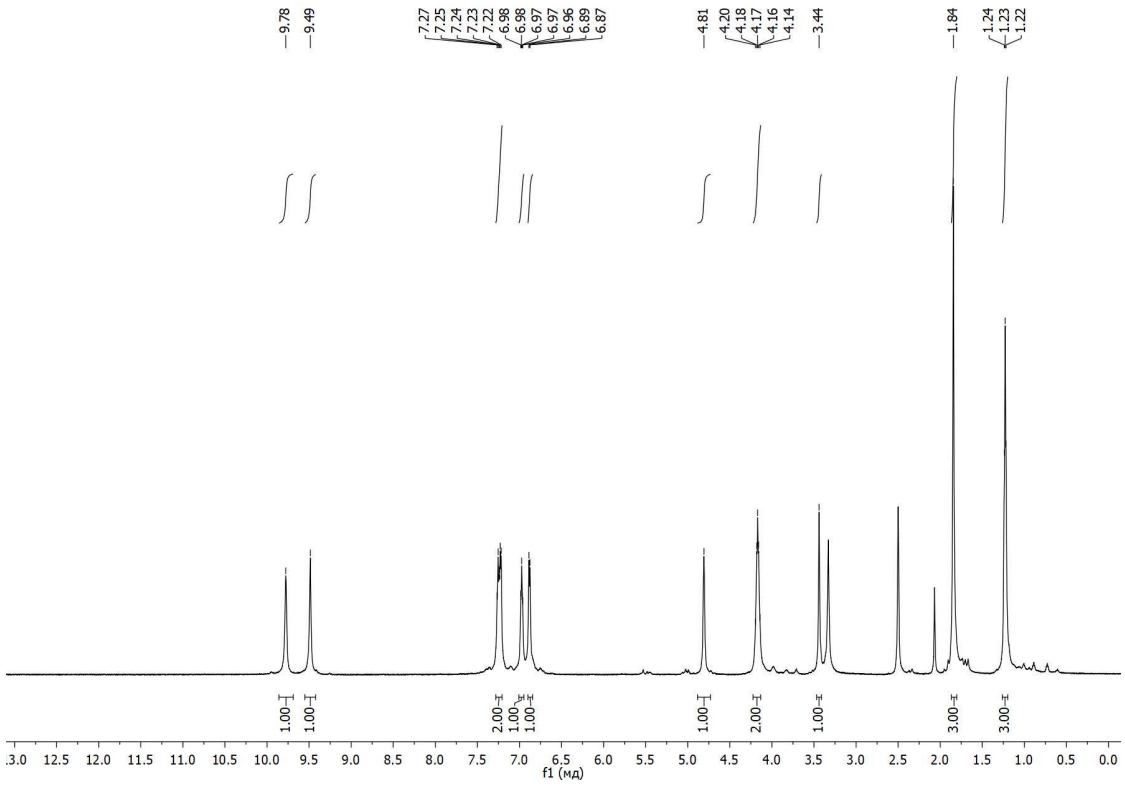

Figure S34. ^{1}H-NMR of bromobis(ethyl 2-methyl-4-thioxo-3,4,5,6-tetrahydro-2*H*-2,6-methanobenzo[*g*][1,3,5]oxadiazocine-11-carboxylate)copper(I), [Cu(L^2)$_2$Br] (6)

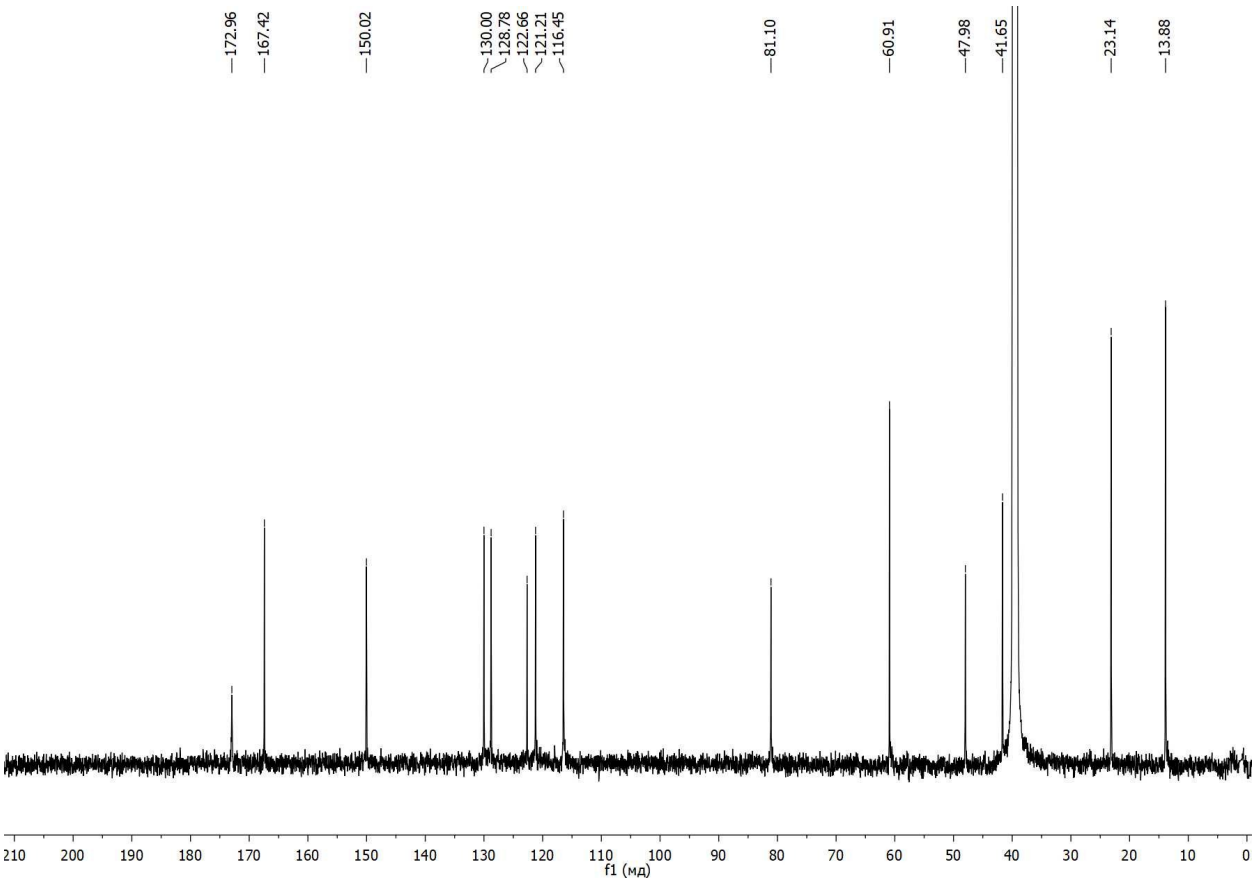

Figure S35. ^{13}C-NMR of bromobis(ethyl 2-methyl-4-thioxo-3,4,5,6-tetrahydro-2*H*-2,6-methanobenzo[*g*][1,3,5]oxadiazocine-11-carboxylate)copper(I), [Cu(L^2)$_2$Br] (6)

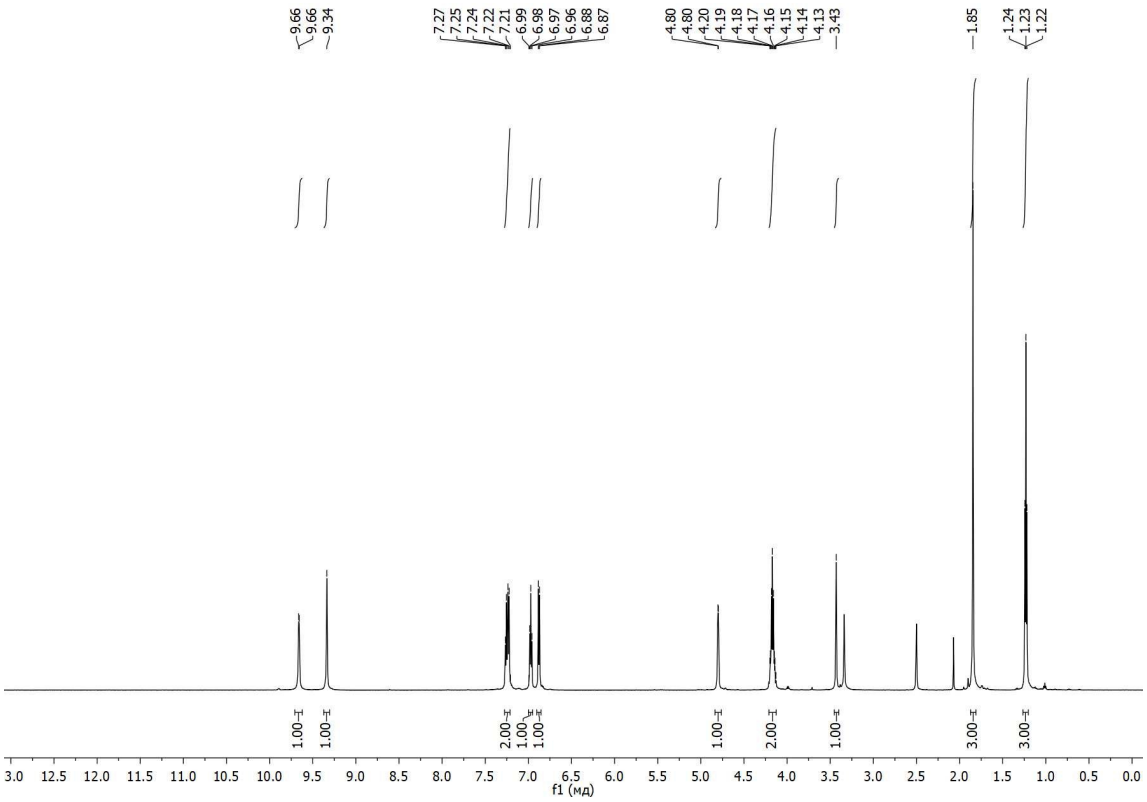

Figure S36. ^{1}H-NMR of iodobis(ethyl 2-methyl-4-thioxo-3,4,5,6-tetrahydro-2*H*-2,6-methanobenzo[*g*][1,3,5]oxadiazocine-11-carboxylate)copper(I), [Cu(L^2)$_2$I] (7)

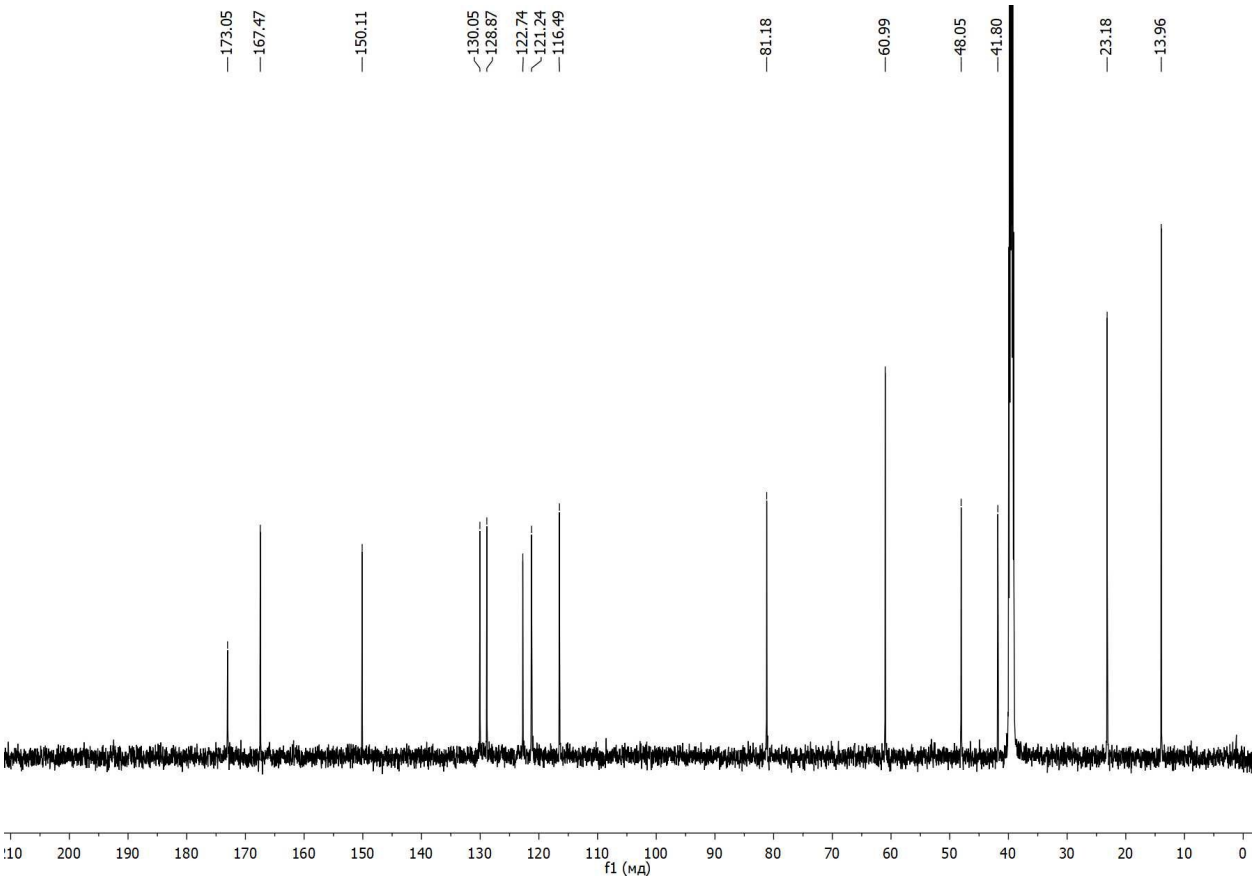

Figure S37. ^{13}C-NMR of iodobis(ethyl 2-methyl-4-thioxo-3,4,5,6-tetrahydro-2*H*-2,6-methanobenzo[*g*][1,3,5]oxadiazocine-11-carboxylate)copper(I), [Cu(L^2)$_2$I] (7)

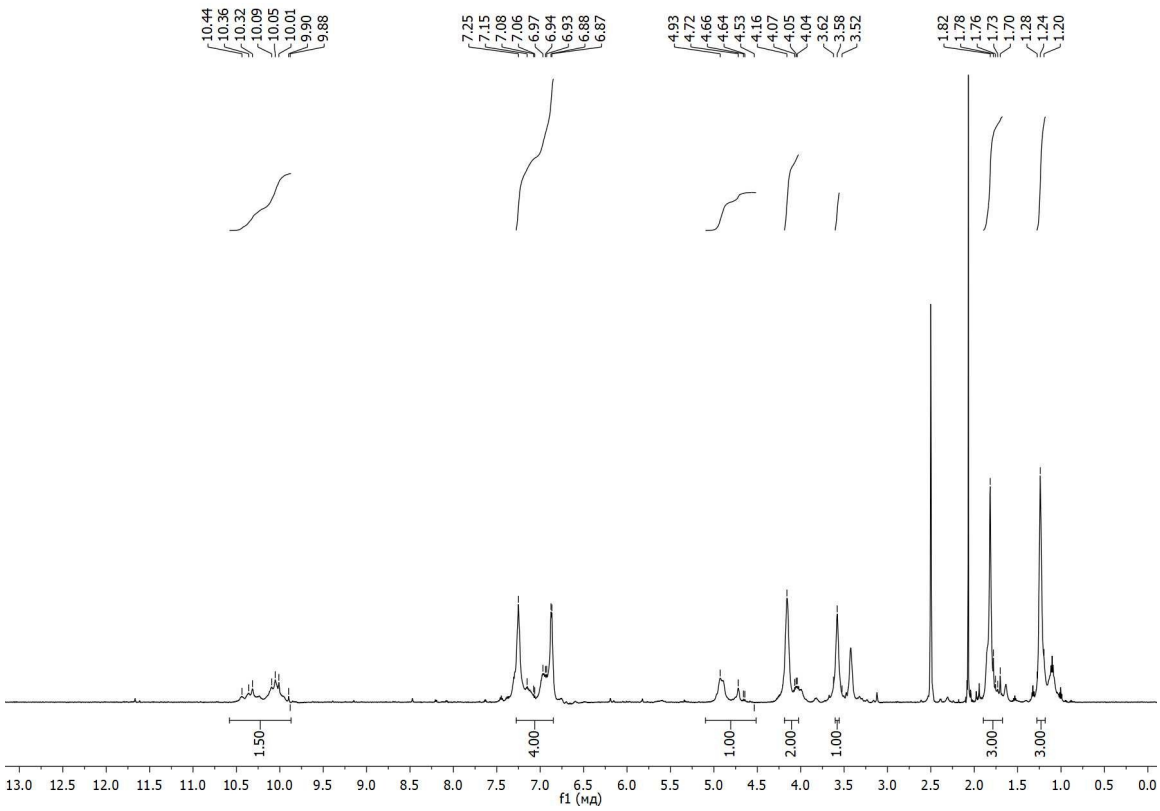

Figure S38. ^{1}H-NMR of dichlorobis(ethyl 2-methyl-4-thioxo-3,4,5,6-tetrahydro-2*H*-2,6-methanobenzo[*g*][1,3,5]oxadiazocine-11-carboxylate)palladium(II), $[Pd(L^2)_2Cl_2]$ (8)

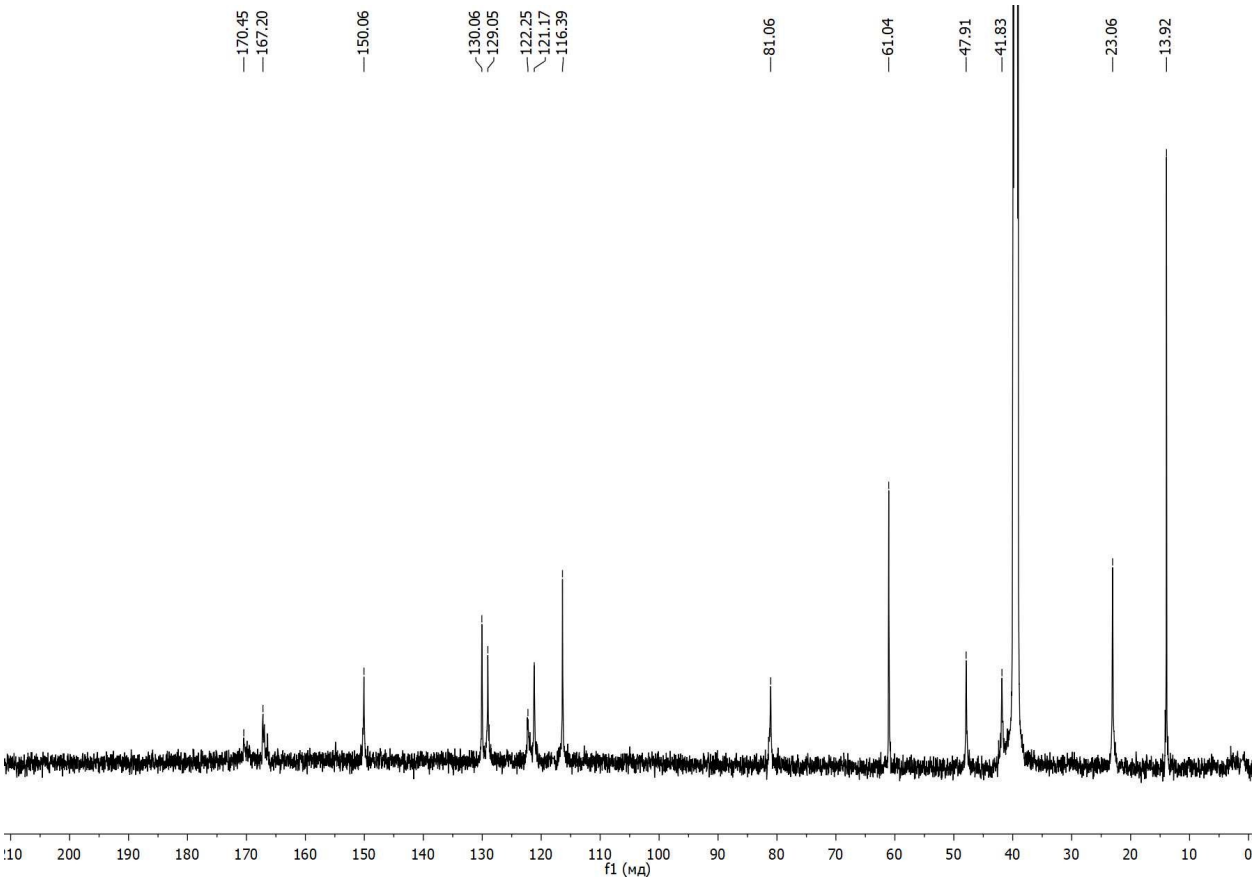

Figure S39. ^{13}C-NMR of dichlorobis(ethyl 2-methyl-4-thioxo-3,4,5,6-tetrahydro-2*H*-2,6-methanobenzo[*g*][1,3,5]oxadiazocine-11-carboxylate)palladium(II), $[Pd(L^2)_2Cl_2]$ (8)

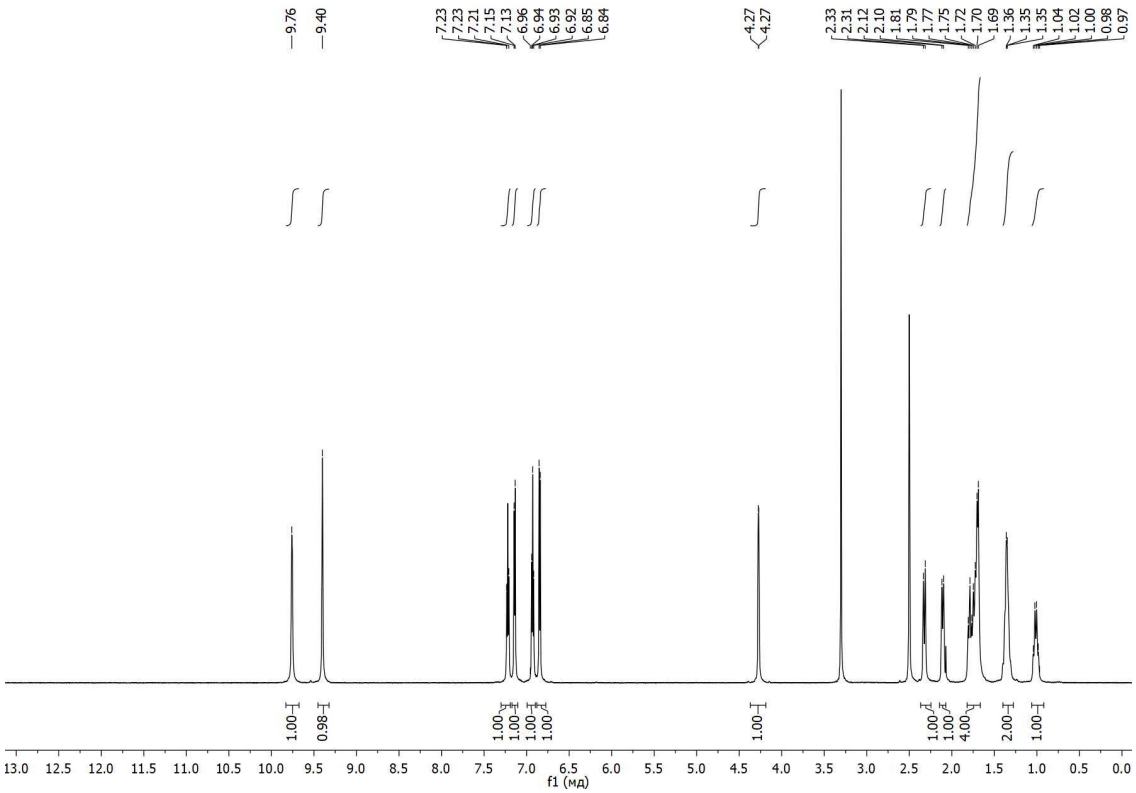

Figure S40. ^{1}H-NMR of chlorobis(1,2,3,4,9,9a-hexahydro-4a,9-(epiminomethanoimino)xanthene-12-thione)copper(I), [Cu(L^3)$_2$Cl] (9)

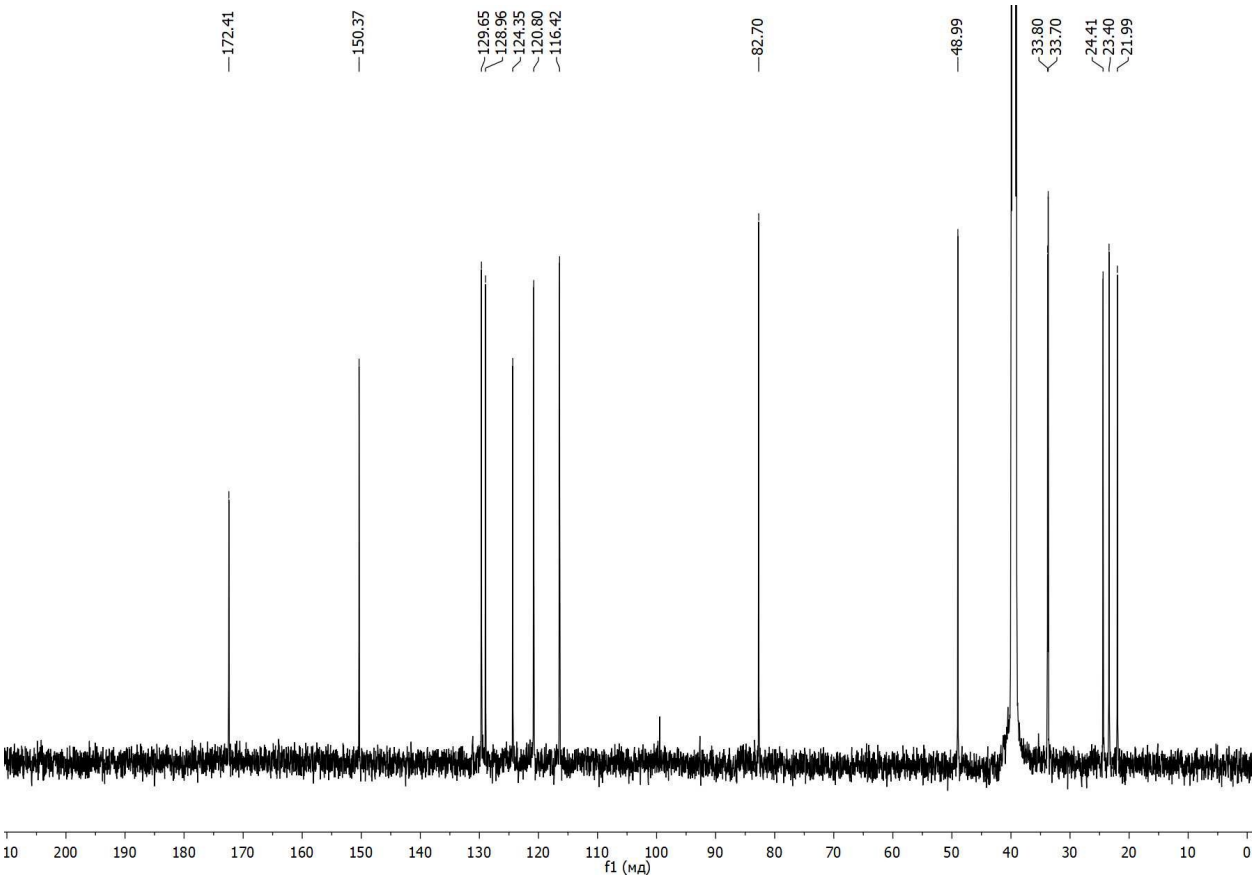

Figure S41. ^{13}C-NMR of chlorobis(1,2,3,4,9,9a-hexahydro-4a,9-(epiminomethanoimino)xanthene-12-thione)copper(I), [Cu(L^3)$_2$Cl] (9)

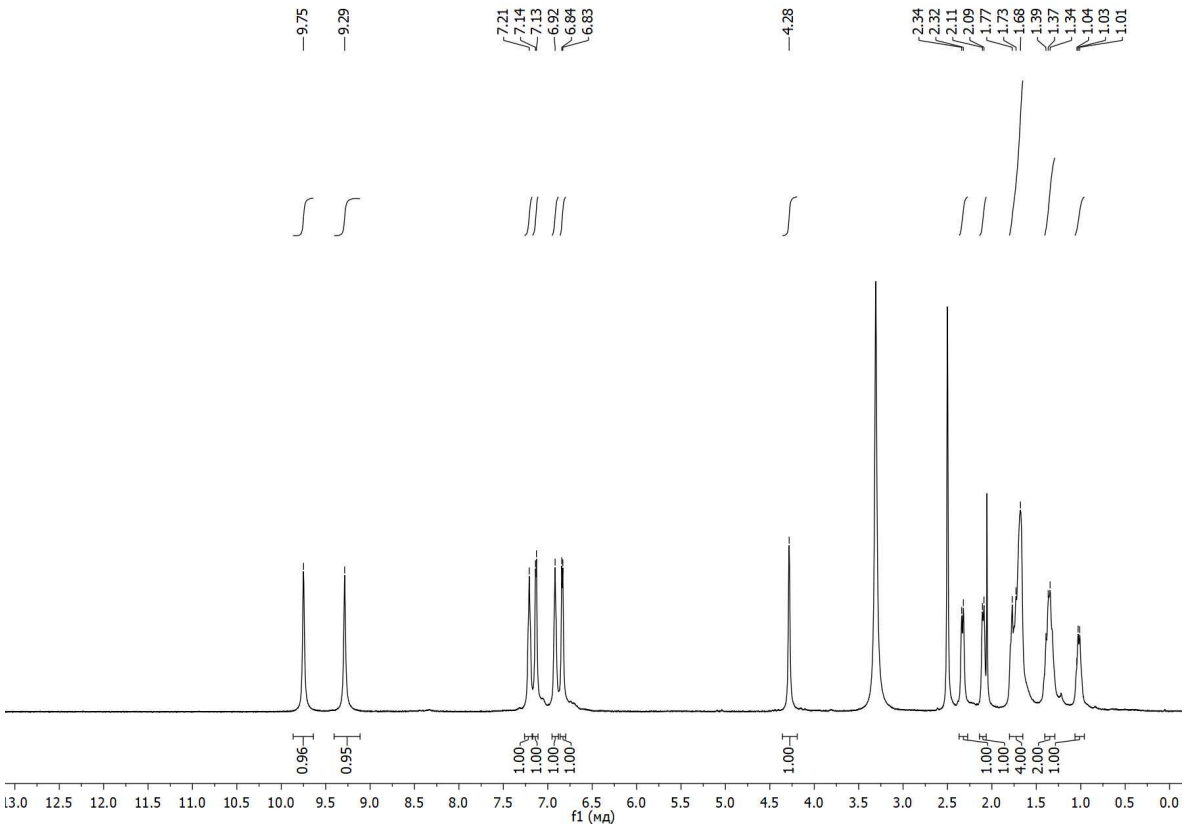

Figure S42. ^{1}H-NMR of bromobis(1,2,3,4,9,9a-hexahydro-4a,9-(epiminomethanoimino)xanthene-12-thione)copper(I), [Cu(L^3)$_2$Br] (10)

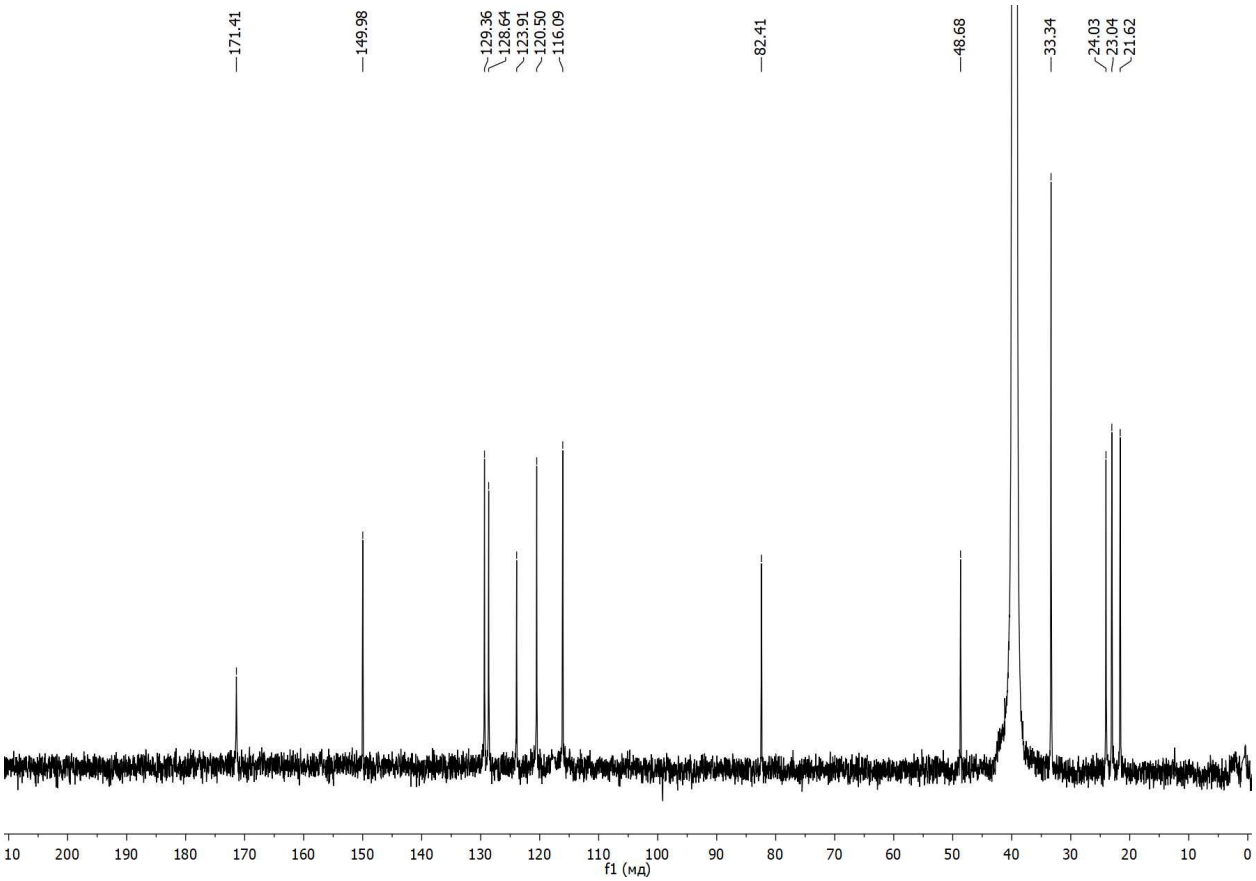

Figure S43. ^{13}C-NMR of bromobis(1,2,3,4,9,9a-hexahydro-4a,9-(epiminomethanoimino)xanthene-12-thione)copper(I), [Cu(L^3)$_2$Br] (10)

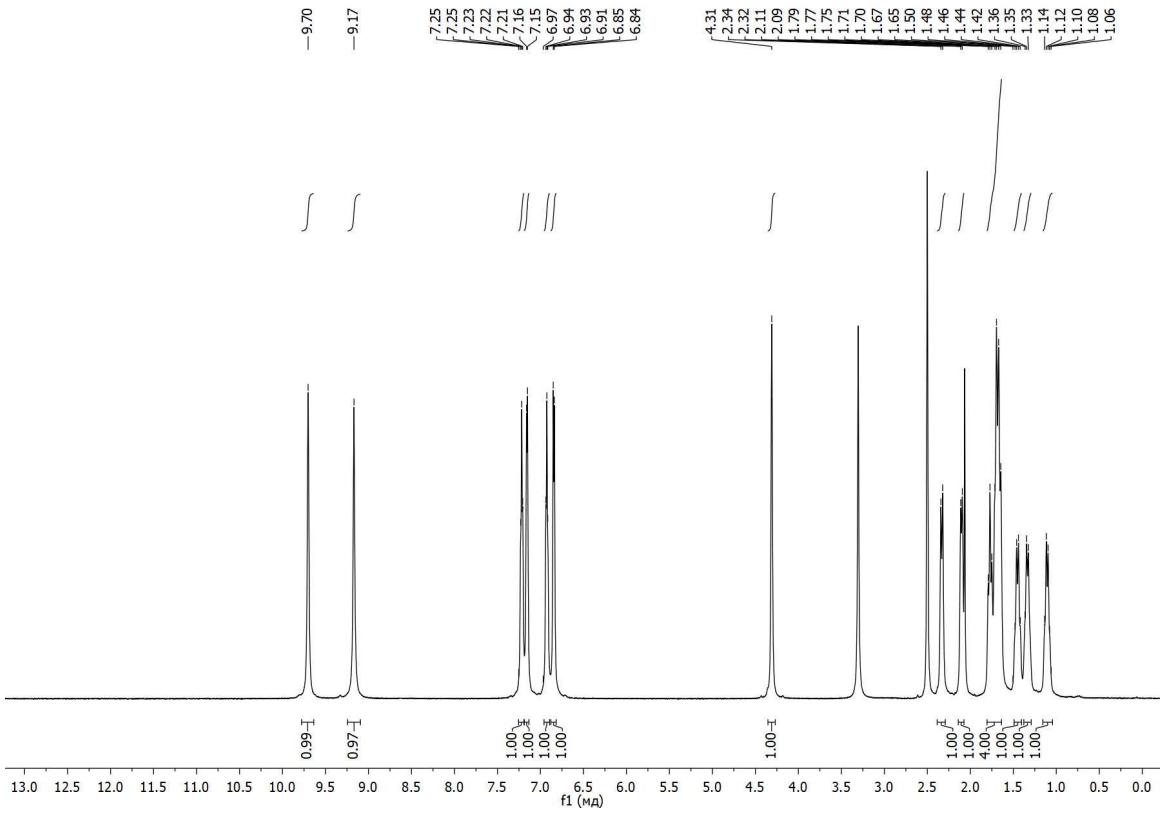

Figure S44. ^{1}H-NMR of iodobis(1,2,3,4,9,9a-hexahydro-4a,9-(epiminomethanoimino)xanthene-12-thione)copper(I), [Cu(L^3)$_2$I] (11)

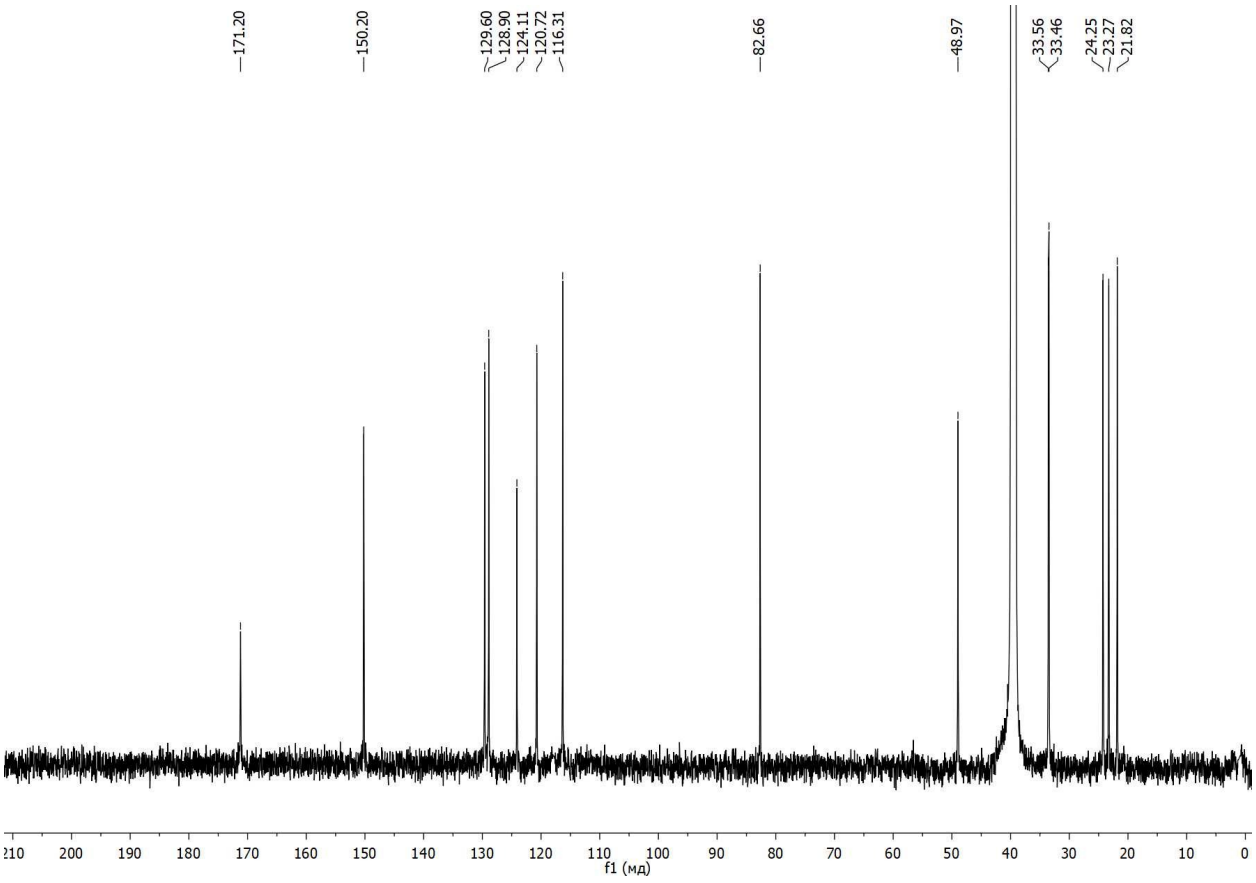

Figure S45. ^{13}C-NMR of iodobis(1,2,3,4,9,9a-hexahydro-4a,9-(epiminomethanoimino)xanthene-12-thione)copper(I), [Cu(L^3)$_2$I] (11)

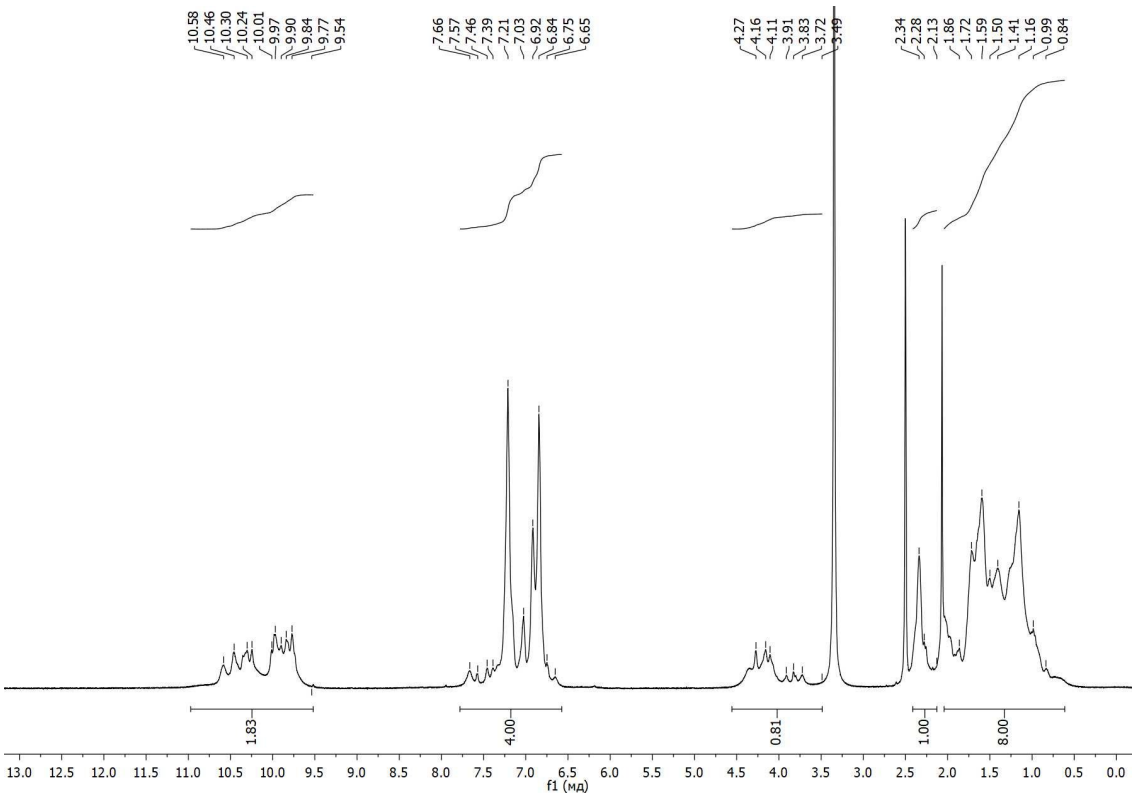

Figure S46. ^{1}H-NMR of dichlorobis(1,2,3,4,9,9a-hexahydro-4a,9-(epiminomethanoimino)xanthene-12-thione)palladium(II), $[Pd(L^3)_2Cl_2]$ (12)

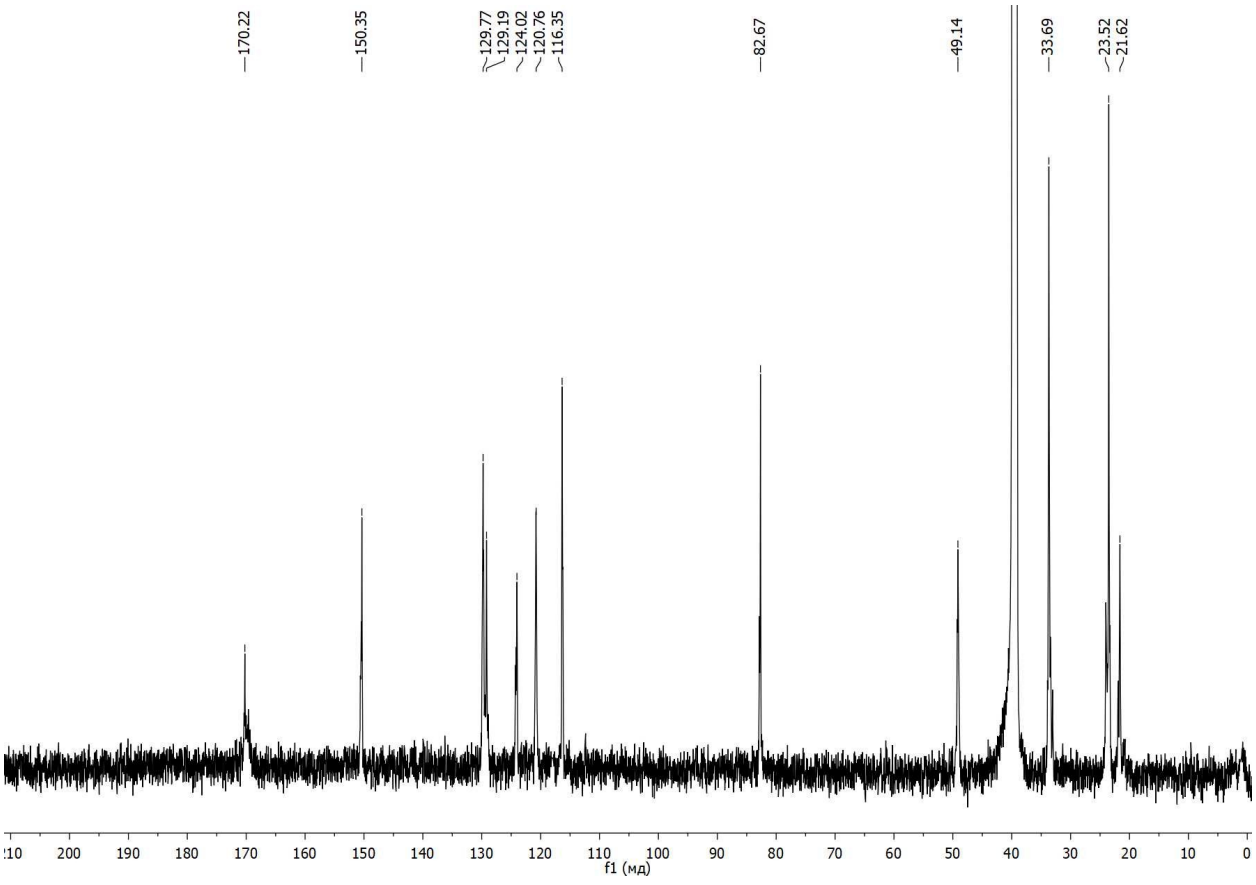

Figure S47. ^{13}C-NMR of dichlorobis(1,2,3,4,9,9a-hexahydro-4a,9-(epiminomethanoimino)xanthene-12-thione)palladium(II), $[Pd(L^3)_2Cl_2]$ (12)

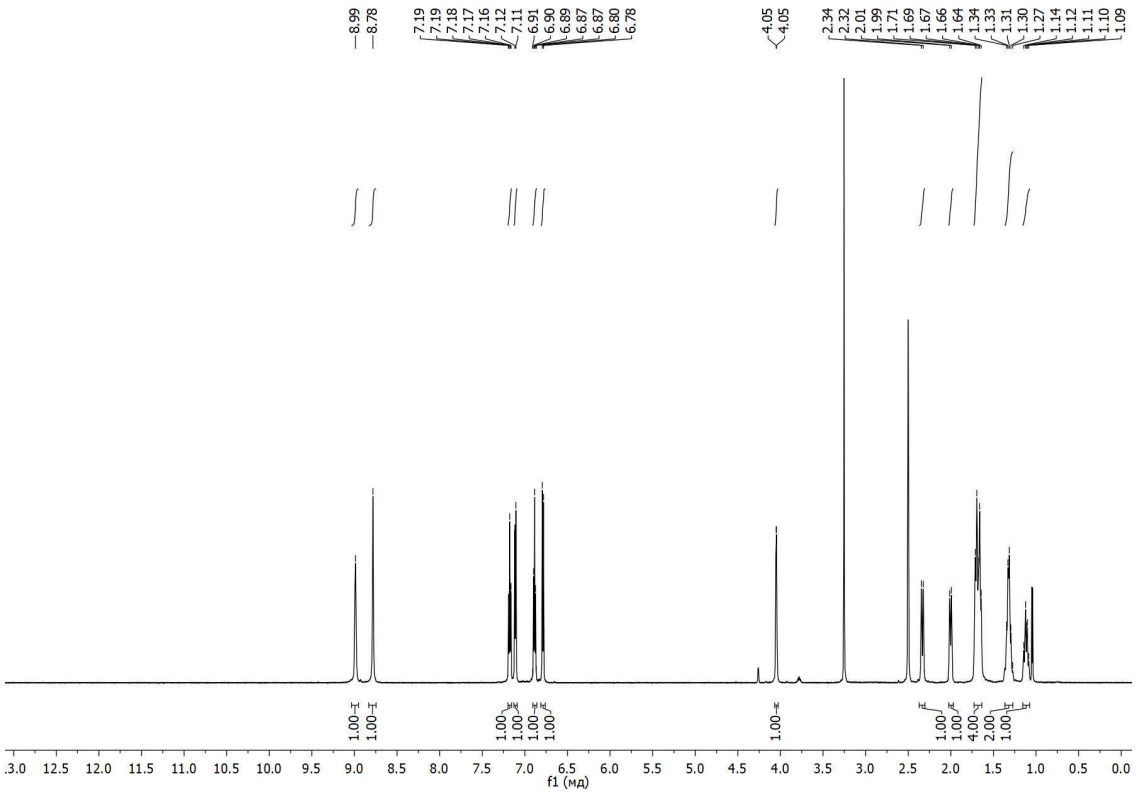

Figure S48. ^{1}H-NMR of 1,2,3,4,9,9a-hexahydro-4a,9-(epiminomethanoimino)xanthene-12-thione (L^3)

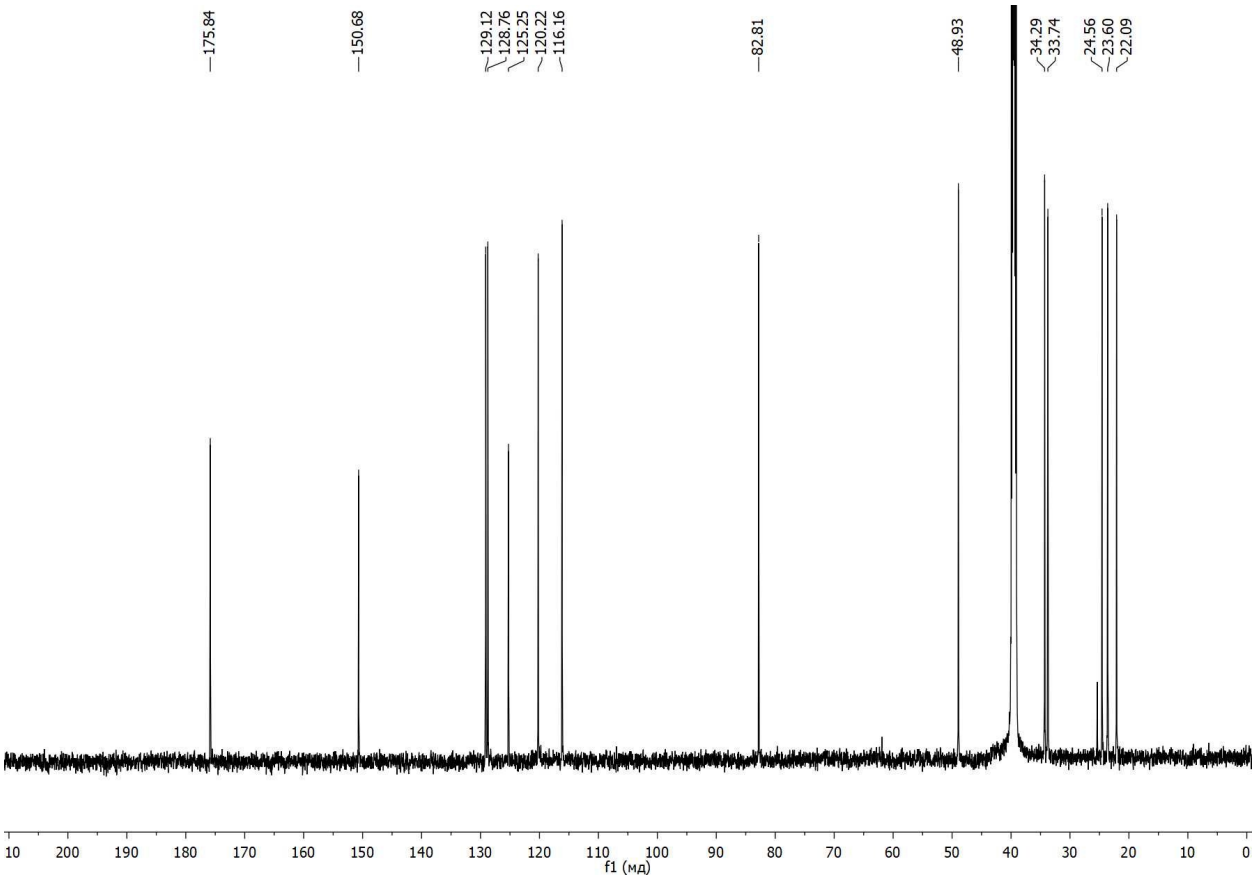

Figure S49. ^{13}C-NMR of 1,2,3,4,9,9a-hexahydro-4a,9-(epiminomethanoimino)xanthene-12-thione (L^3)

References

1. I. V. Kulakov, S. A. Talipov, Z. T. Shulgau, T. M. Seilkhanov, *Chem. Heterocycl. Compd.* **2015**, *50*, 1478–1486.
2. A. Mobinikhaledi, N. Foroughifar, T. Mosleh, A. Hamta, *Phosphorus. Sulfur. Silicon Relat. Elem.* **2012**, *187*, 728–734
3. G. M. Sheldrick, *Acta Crystallogr. Sect. C Struct. Chem.* **2015**, *71*, 3–8
4. A. L. Spek, *Acta Crystallogr. Sect. D Biol. Crystallogr.* **2009**, *65*, 148–155
5. C. F. Macrae, P. R. Edgington, P. McCabe, E. Pidcock, G. P. Shields, R. Taylor, M. Towler, J. van de Streek, *J. Appl. Crystallogr.* **2006**, *39*, 453–457.
6. a) E. V. Savinkina, I. A. Zamilatskov, A. S. Kuzovlev, D. V. Albov, D. V. Golubev, V. V. Chernyshev, *Polyhedron* **2014**, *69*, 68–76; b) S. G. Zhukov, V. V. Chernyshev, E. V. Babaev, E. J. Sonneveld, H. Schenk, *Zeitschrift für Krist. - Cryst. Mater.* **2001**, *216*, 5–9; c) V. B. Zlokazov, V. V. Chernyshev, *J. Appl. Crystallogr.* **1992**, *25*, 447–451; d) S. V. Andreev, S. A. Zverev, I. A. Zamilatskov, N. M. Kurochkina, G. V. Ponomarev, A. N. Fitch, V. V. Chernyshev, *Acta Crystallogr. Sect. C Struct. Chem.* **2017**, *73*, 47–51; e) D. R. Erzina, I. A. Zamilatskov, N. M. Stanetskaya, V. S. Tyurin, G. L. Kozhemyakin, G. V. Ponomarev, V. V. Chernyshev, A. N. Fitch, *European J. Org. Chem.* **2019**, *2019*, 1508–1522.